

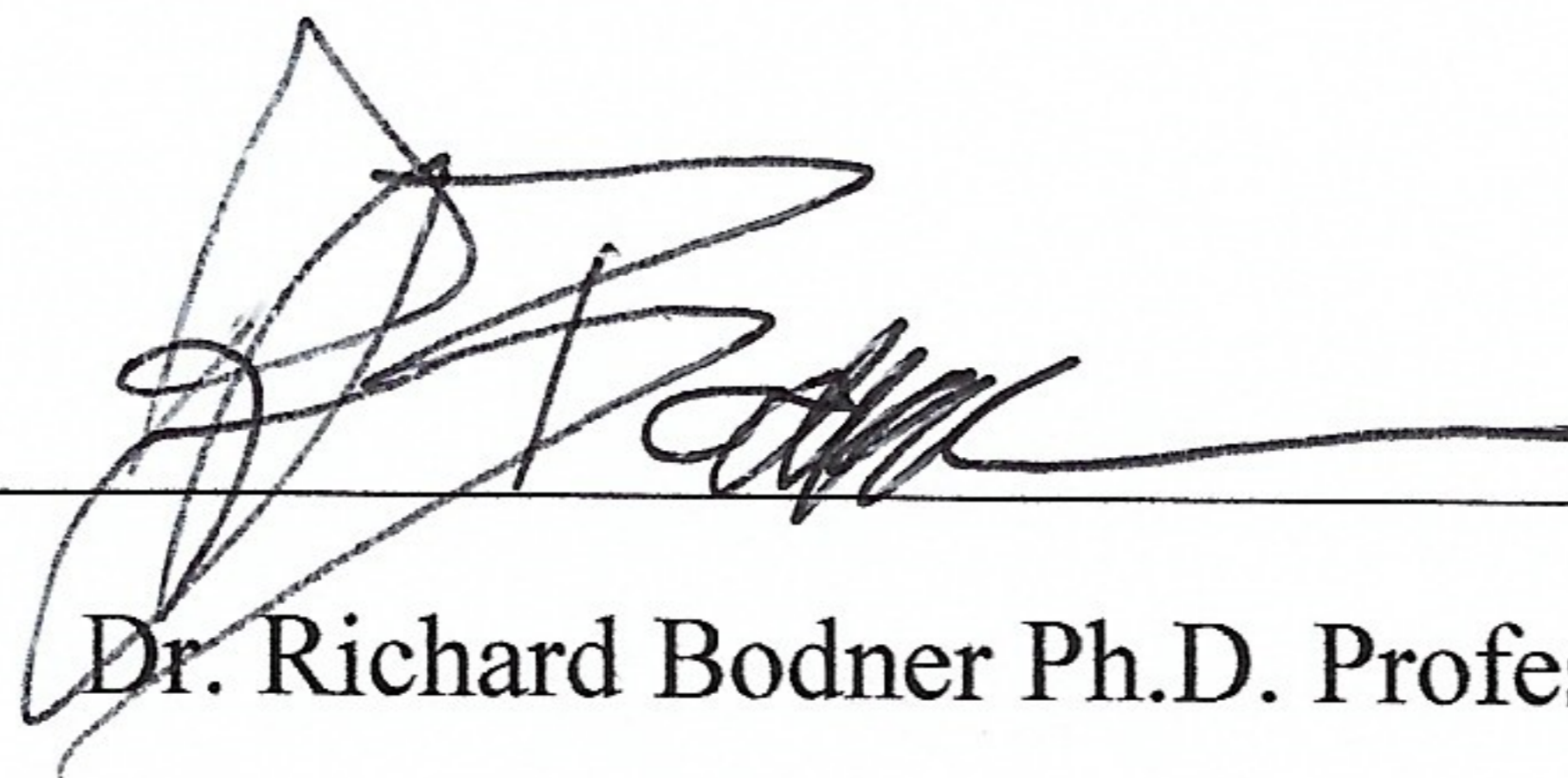
A Quantitative Morphological Analysis of Sensory Deprived Supragranular Neurons in the
Mouse Barrel Cortex

By: Danna Shimuny
City University of New York
Queens College
Mentor: Joshua Brumberg

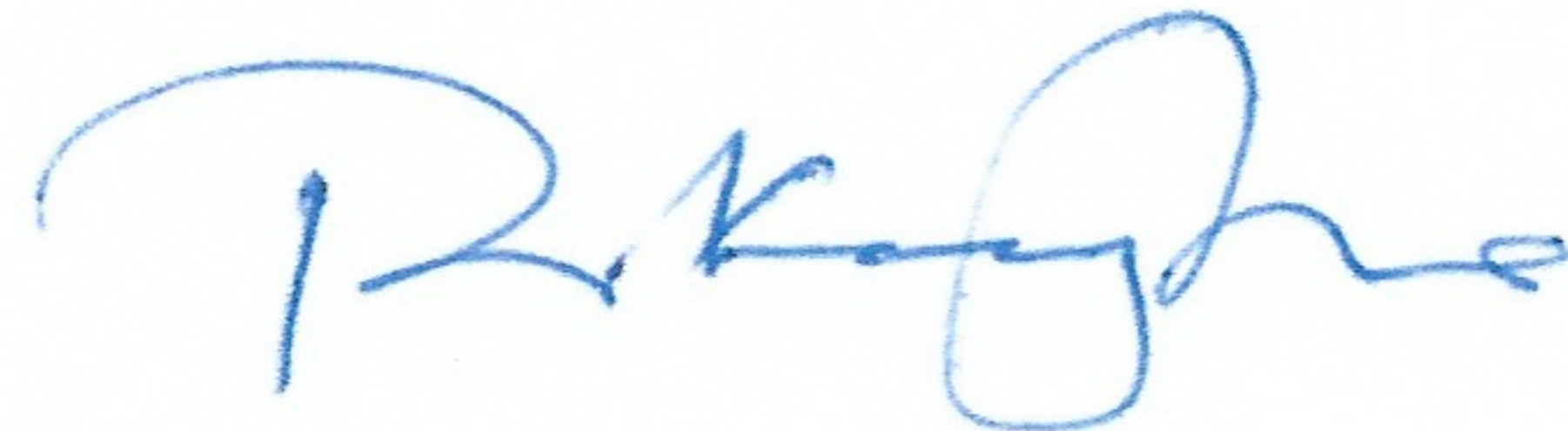
Thesis approval page:

Defended on June 29, 2020

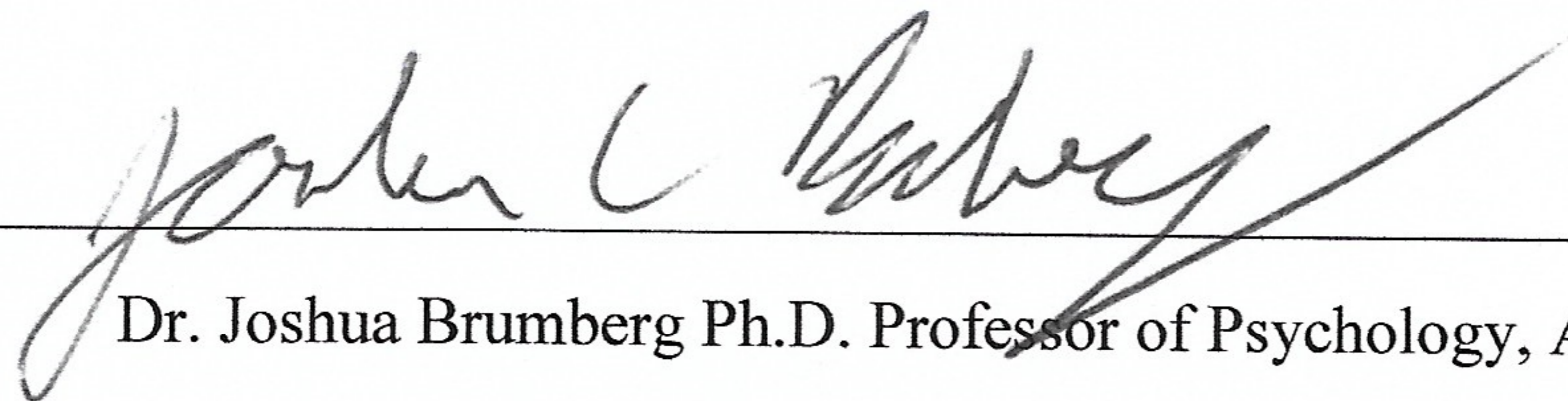
Approved by:



Dr. Richard Bodner Ph.D. Professor of psychology,



Dr. Pokay Ma Ph.D. Professor of Biology



Dr. Joshua Brumberg Ph.D. Professor of Psychology, Advisor

Table of Contents

Abstract.....5

Chapter 1: Introduction 6

 1.1 Background 6

 1.2 Signaling pathway from the primary sensory cortex to layers 2/3..... 7

 1.3 Neuron Morphology of the different layers.....8

 1.4 Relationship between the M1, S1, and S2 cortices.....11

 1.5 Morphological circuit staining12

Chapter 2: Methods and Materials..... **14**

 2.1 Experimental Animals 14

 2.2 Anesthetic procedures and administration 14

 2.3 Fluorescent Bead Labeling.....15

 2.4 Diolistics preparation and labeling.....16

 2.5 Tissue fixation and storage.....18

 2.6 Imaging.....18

 2.7 Reconstruction and Measurements.....19

 2.8 Statistical Analyses.....19

Chapter 3: Results.....21

 3.1 Neuronal Reconstructions.....21

 3.2 Cell Body.....22

 3.2.1 Perimeter.....22

 3.2.2 Area.....23

 3.2.3 Soma Roundness and Form Factor.....24

 3.2.3 Convexity.....26

 3.2.4 Solidity and Compactness.....26

 3.2.5 Feret Min and Feret Max.....28

 3.2.6 Aspect Ratio.....29

3.3 Neuronal Dendrites.....	30
3.3.1 Dendrite Quantity.....	31
3.3.2 Dendrite Nodes.....	31
3.3.3. Dendritic Ends.....	31
3.3.4 Dendritic length and Mean length.....	32
3.3.5 Dendritic complexity.....	33
3.4 Dendritic trees.....	34
3.5 Dendritic tree length.....	36
Chapter 4: Discussion	39
4.1 Results Summary.....	39
4.2 Interpretation of the data.....	41
4.3 Limitations of the study.....	44
Figure Legends	45
Table Legends	50
References	51
Figures	56
Tables	71

Abstract

Rodent primary somatosensory neocortex layers 2 and 3 are important for the propagation of whisker stimuli to adjacent cortical regions. Such stimuli are initially mediated by layer 4 in the barrel cortex and are transmitted to layers 2 and 3. Primarily focusing on the primary somatosensory barrel field (S1BF1) of the barrel cortex and on the projecting neurons from the supragranular layers which connect with the contralateral primary somatosensory cortex (S1), ipsilateral primary motor cortex (M1) and ipsilateral secondary somatosensory cortex (S2). The principle objective of this study was to determine if specific morphological characteristics are associated with each of the projecting neuronal groups S1, M1 and S2. To accomplish this a morphological approach was adopted to analyze supragranular projecting neurons associated with these M1, S1, and S2 circuits and determine the impact of sensory experience on their development. To alter their sensory experience deprivation was induced by whisker trimming. CD-1 mice were used in this study, retrograde bead labeling techniques combined with diolistics to double stain the brain and allow for the identification of projecting neurons allowing for their reconstruction. Once the reconstructions were analyzed it was found that the target M1, S1, S2 sensory deprived target cells had soma that were smaller and less round than control cells. They also exhibited shorter dendrites as compared to the callosal cells as well as the development of the dendritic tree being smaller.

Chapter 1

Introduction

1.1: Background:

Rodents such as mice and rats use whiskers, which are highly sensitive detectors for tactile information, to assess their surroundings. Their whiskers allow them to construct spatial representations of their environment, locate objects, and discriminate fine grain textures (Diamond et al., 2008). The barrel cortex is the region of the rodent brain that processes the somatosensory signals originating from the whiskers (Woolsey et al., 1975). Somatosensory processing of whisker-related environmental information is highly structured into stereotypical maps that occupy a significant portion of the rodent brain, this can be referred to as the barrel map (Feldman, 2005). Barrels, which are prominent sensory units in the somatosensory cortex of rodents are one of the salient features of neocortical development since they form specific topographic maps in which neighboring neurons can receive input relayed from sensory afferents (Inan & Crair, 2007). The barrel map is genetically determined to a large extent and forms early in life. The map is set within a few days of birth, so that even drastic treatments, like peripheral lesions, have little effect on the somatotopic layout of the barrels after the first few days of life (Peterson, 2007). There is a direct multi-synaptic pathway from the rodent whisker to the barrel cortex, with each whisker having a particular place in the barreloid, located in the thalamus (Li & Crair, 2011).

The rodent somatosensory system is an excellent model system when it comes to the study of sensory function and development into maturity. Motor control is involved in moving the whiskers during object exploration and palpation, frequently performing rapid rhythmic

sweeping motions of large amplitude, and thus this sensory system is an attractive model for investigating sensorimotor integration and active sensory processing (Zagha et al., 2013).

Whisker trimming in newborn mice can show how the primary somatosensory cortex develops and adapts over the rodent life span, sensory deprivation can result in adaptations in the cortical anatomy (Micheva & Beaulieu, 1995). Studies have shown that the primary somatosensory barrel field or S1BF1 region of the mouse brain, has the capacity for anatomical reorganization of neuronal cells. Specifically, sensory deprivation through whisker trimming impacts dendritic development such as dendritic length, bifurcation, quantity, and complexity as well as soma area, perimeter, complexity etc. (Peterson 2004). Neuronal alterations in the cortical receptive field can be produced in the rodent brain after a few days of trimming whiskers in neonatal mice (Kelly et al., 1999).

1.2 Signaling pathway from the primary sensory cortex to layers 2/3:

The organization of the primary sensory cortex ($\bar{S}I$) can be seen in the arrangements of mouse whiskers, as each whisker represents a barrel in layer 4 of the contralateral primary somatosensory cortex (Lübke et al., 2003). When rodents explore their surroundings, they use the whiskers on their snouts to further explore and learn. These signals will then travel through the circuits that are in the rodent's whisker follicles. In response to the whisker signaling, mechanosensitive ion channels at the nerve endings will open and depolarization will occur. This depolarization will then activate the deep fiber neurons located in the infraorbital branch of the trigeminal nerve (Figure 1). Next, it will send that signal to the brainstem intended for further processing of the whisker inputs (Dimond, 2012) [reference?]. The signaling pathway from the brainstem then involve second order neurons that carry the signal further to the ventral posterior

medial (VPM) nucleus in the thalamus. From there, the sensory information gets transmitted via the thalamocortical afferent to the primary somatosensory cortex barrel field (S1BF) on the ipsilateral side. The major recipient area in S1BF1 for information from VPM is layer 4, also known as the granular layer. Sensory information then travels to the rest of the cortical column, first reaching the supragranular layers 2/3, then on to the infragranular layers 5/6, the layers responsible for connecting the neocortex to other subcortical structures (Petersen & Crochet, 2013). Each of these cortical layers contain a heterogenous population of neurons, either physiologically (e.g., de Kock et al., 2007), biophysically, (Ferrante et al., 2017), or morphologically (Narayanan et al., 2015). Focusing on the pyramidal cells in Layers 2/3, whisker signaling will then be further processed to the other areas of the contralateral or ipsilateral areas of the cortex. Neurons from layers 2/3 in the barrel cortex project to the ipsilateral motor cortex (M1), contralateral primary somatosensory cortex (S1), and the ipsilateral secondary somatosensory cortex (S2) among other areas (Feldmeyer, 2012).

1.3 Neuron Morphology of the Different Layers:

Neurons are grouped into respective circuits for processing of neuronal signaling to the correct brain regions. Neuronal morphology plays a role in how well a signal can be transmitted thus making it crucial to the communication and functioning between the neurons and their locations. For example, neurons located in layer 4 can be described as star-like cells based on their morphology. They have dendrites which are multipolar as opposed to layer 2/3 pyramidal cells which have bipolar dendrites. Layer 4 cells are connected to other layer 4 neurons via dense synaptic interconnections within the barrel. Layer 4 neurons also have cell bodies (somata) that are spherical in shape and also have the capacity to vertically cross the barrel perimeter to synapse onto supragranular neurons (Lübke et al., 2003). The next layer, Layer 5, has two

different types of pyramidal neurons, one principal type are the corticostriatal neurons, which project to the striatum, and they are typically thin tufted pyramidal neurons. The second type of layer 5 pyramidal neurons project to posterior nucleus of the thalamus, superior colliculus, brainstem, and the pons (Alloway, 2007), and typically have thick apical tufts. Both these neurons represent canonical elements of the cortical circuitry due to their presence across the cortical areas such as the somatosensory, motor, auditory, visual and the prefrontal cortices (Oberlaender et al., 2011). Studies conducted on the supragranular layers or layer 2/3, have demonstrated that the neurons contained within the supragranular layer are primarily composed of pyramidal neurons. Traditionally, pyramidal neurons can exhibit morphological heterogeneity through both their apical and basal dendritic branching patterns (Lübke, 2003). These dendrites can differ in the length and width of their bifurcating apical tuft. Similarly, their basal dendrites also differ in both length, order, or the location of bifurcation in their dendrites. In addition, the neurons found in these layers will present diversity in their axonal lengths giving the cells the capacity to influence their projecting patterns to the adjacent cortical areas (Feldmeyer 2012). Understanding, the orientation of pyramidal basal dendrites and their connection to the stellate cells contained within the barrel cortex can show a better understanding of how these neurons send and receive signals to other cortical layers through the observation of their morphology and orientation (Alexander & Hasselmo, 2018). In turn, this mechanism of neuronal signaling can relay processed whisking sensations from layer 4 to the supragranular layers. In addition, pyramidal neurons and their long axons, neuronal signaling may travel through to areas such as the M1, S1, and S2 (Holmgren et al., 2003). Therefore, layer 4 neuronal cells are connected to layer 2/3 cells through their basal dendrites and under sensory deprived conditions, the dendritic lengths as well as dendritic quantity could affect how these neurons interact with one another.

Pyramidal cells in layer 2/3 have a substantial horizontal dendritic reach, these cells undergo long term potentiation at a greater dendritic complexity in the horizontal direction with slightly greater horizontal reach than those that did not experience change in the strength of the synapse. In the control cortex, it is found that only one third of layer 2/3 neurons exhibit changes in their synaptic inputs in response to some paradigm (Ismailov 2004). Additionally, cells in the sensory deprived condition can be found with similar dendrites from different deprivation groups, which showed the same plasticity. Studies have found that deprivation substantially shifted plasticity from depression to potentiation without influencing dendritic arborization. Furthermore, the sensory experience will have a substantial control in influencing plasticity on layers 2/3. While synapses depressed by whisker trimming have been shown to have a higher probability of potentiating and a greater magnitude of potentiation (Allen et al., 2003; Hardingham et al., 2008; Hardingham et al., 2011).

Layer 4 neurons influence neurons in layers 2/3, though direct synaptic connections, whisker trimming not only impacts layer 4 but also influences neurons in layer 2/3 (Margolis et al., 2012), the firing of layer 2/3 pyramidal neurons in the deprived cortex have been altered due to change in the spike timing primarily seen in neurons that have responded poorly to whisker-trimming (Albieri et al., 2015). Rodent developmental studies have noted whisker trimming impacts layer 2/3 of the barrel cortex in a multitude of ways. Sensory deprivation can cause anatomical reorganizations of layers 2/3, 12 to 14 days after birth has been found to be the critical period for the development of neurons in these layers (Stern et al., 2001). Thus, altering them through sensory deprivation techniques such as whisker trimming should show some impact on the neuronal cells in these layers.

1.4 Relationship between the M1, S1 and S2 cortices:

In rodents, environmental information is conveyed to the sensory areas of the cortex being registered then encoded as perceptual information. The animal can then make a suitable motor adjustment in response to its surroundings. This indicates there is a relationship of the motor system and the somatosensory systems between the motor (M1) cortex and the somatosensory (S1) cortex in the mouse brain (Ferezou et al., 2007). There is a close relationship in the amount of sensory fields or sensory cortexes a mammal can have and its complexity seen in its behavior and sensory processing, the more sensory cortexes the more complex information the animal can extract from its direct environment (Kaas, 2000; Santiago et al., 2019). It has been shown that each of the sensory areas has the capacity to extract different information from the environment as well as organize it to its respective cortexes appropriately. The motor circuit provides purposeful movements as a response from sensory inputs hence the interconnected S1 and M1 cortexes are important for motor planning (Metzner & Juranek, 1997; Santiago et al., 2019). When a mouse is encountering a new environment, it explores it using its whiskers. The whiskers have a one-dimensional range of movement, moving forwards and backwards. Studies have shown that whisker movements can be evoked through the direct stimulation of the neurons located in the primary whisker motor cortex (M1)(Ferezou et al., 2007). Another study, has shown that sensory signals to the motor cortex originate from the somatosensory cortex (S1) and the thalamus (Alloway et al., 2004). Furthermore, the whisker motor cortex can serve to combine sensory information with voluntary motor commands (Friedman et al., 2012). This indicates that there is a relationship between the S1 cortex and the

M1 cortex in respect to a rodent's sense of touch through simple whisker movement. *In vitro* physiologic data have also shown that the primary motor cortex and the primary somatosensory cortex are paired mono-synaptically (Mao et al., 2011; Rocco-Donovan et al., 2011).

Secondary somatosensory (S2) cortex receives input from the sensory associated thalamic nuclei (VPL and VPM) and the medial ascending systems from the contralateral thalamus. It is primarily involved in spatially directed attention towards pain (Aghion & Rees Cosgrove, 2014). The S2 cortex can be considered to have a role in multisensory integration with the primary somatosensory cortex (Menzel & Barth, 2005), the S1-S2 circuit is believed to be responsible for higher order perception of stimuli input. The primary motor cortex has the capacity to relay information to the S1-S2 circuit. Studies have shown that this interaction could result either from a cortico-thalamocortical pathway or a common drive of the shared areas. Mainly focusing on S1_{S2} and S2_{S1} cortexes and their respective neurons will become active during whisker-texture touch. Interestingly, when the motor behavior are paired with the sensory stimuli interactions more likely represent the exchange of sensory- or decision-related activity (Chen et al., 2016). This implies that the motor cortex may control the efficiency of the S1-S2 circuit in times of rodent exploration.

1.5 Morphological circuit staining:

Studies investigating the neuronal morphology within the barrel cortex have traditionally utilized the Golgi-Cox staining techniques (Woolsey, 1975). Better methods of staining have evolved due to better time efficiency and a direct staining method for capturing neurons (Kim et al., 2007). More recently, retrograde-labeling fluorescent beads (Katz et al., 1984; Kim et al., 2007; Schofield, 2008) have been used as an effective method in tracing cortical circuits, along with diolistics labeling (Gan et al., 2000). Diolistics staining is a relatively new method of

labeling cells, using lipophilic fluorescent dyes such as dialkylcarbocyanine (DiI, see methods section). Since this type of fluorescent dye is lipophilic it diffuses through the neuronal membrane and stain the cell in its entirety, including soma and dendrites (Schofield, 2008). Fluorescent bead labeling can be retrogradely transported through the synapse to label the presynaptic neuron, staining the cell body. Overall, this staining method can reveal a neuron that is associated with a specific projection site and circuit (Katz et al., 1984).

The purpose of the current study is to determine the influence of sensory deprivation on the supragranular projection cells within the barrel cortex of CD-1 mice. With callosal cells exhibiting the typical morphology of neuronal cells. M1 projecting cells in the S1BF1 region can have a traditionally pyramidal cell shape or a stellate cell body with long dendrites. S1 projecting cells have elongated oblong soma bodies and lastly S2-projecting cells have a more spherical soma with long dendrites(Palaguachi 2017). The morphology of the different neuronal phenotypes was dramatically impacted by sensory deprivation. As seen in Figure 6A, M1 neurons had a more spherical soma, with shorter dendritic length deprived of their normal sensory inputs via whisker trimming. Figure 6B shows the S1 pyramidal cells following sensory deprivation had more triangular shaped somas with longer dendrites. Lastly, in figure 6C, S2 cells had an elongated oblong triangle cell body with fewer dendrites that were longer following sensory deprivation. In sum, sensory deprivation via whisker trimming of CD-1 mice has resulted in morphological changes. The purpose of this study is to determine if the supragranular projection neurons will display morphologies that are unique to their projection site and it is proven by the experiment done in this current study of the supragranular layers of the rodent brain.

Chapter 2

Methods and Materials

2.1. Experimental Animals:

CD-1 mice (Charles River Laboratories) were used for all the experimental procedures. Mouse pups of both sexes were obtained from 6 pregnant mice. The pregnant mice were randomly assigned into either the control or trim conditions with the investigator not blinded to the condition. As a result, the pregnant mouse's pups were placed under the same experimental conditions, assigned to either control group or experimental groups totaling 7 male and 8 females. The mice were reared in the Queens College, CUNY, animal facility and allowed *ad libitum* access to food and water. Male and female mice were caged separated at P18, with 3-4 mice per cage. Post-surgical mice were housed individually and were monitored by a research assistant. All experiments were conducted in accordance with Queens College's animal use policies and were approved by the Institutional Animal Care and Use Committee (IACUC, protocol #100).

2.2. Anesthetic procedures and administration:

To anesthetize the mice for surgery, ketamine/Xylazine solution (0.50mL of Xylazine, 1.18mL of Ketamine dissolved in 10 mL of 0.9% saline) were injected intramuscularly. The dose was dependent on the weight of each mouse; a mouse weighed 50g, it would be given 0.5mg/kg of anesthetic for surgery. If the mouse weighed less than 50g then the proper adjustments were made to give the correct dose of anesthetic. All mice were first weighed so that the anesthesia was customized to the weight of each animal. Intramuscular injections are the choice over intraperitoneal injections because this type of injection used a 30G ½" long needle and was administered through the thigh and the anesthetic effect lasted slightly longer than intraperitoneal

injections and it allowed for fewer booster shots during surgeries, even though it may take slightly longer for the anesthesia to take effect compared to intraperitoneal injections. After the mouse becomes unresponsive to a noxious stimulus (toe pinch), the surgery starts. Reflexes were checked every 5 minutes and booster shots (0.1mL) were administered as needed.

2.3. Fluorescent Bead Labeling:

CD-1 mice in the control group were used to establish a baseline of the target neurons while mice in the experimental group underwent whisker trimming on both sides of their snout from postnatal day (P)0 to P30. With the use of Micro-scissors, the whiskers were clipped close to the base of the follicle, every other day consistently from the first day of life until 30 days after birth. Animals in both the control and sensory deprived conditions were exposed to the exact same conditions in terms of bedding texture, food and water source, anesthesia, and handling. The control animals were also handled, anesthetized, and returned to the cage on the same trimming session as the sensory-deprived animals(Chen et al., 2014). Surgeries were done using a stereotaxic device (David Kopf Inc.), which held the mouse in place while it rested on a heating pad (Fine Science Tools) to prevent the loss of body heat. Once correctly positioned, the hair on the skull was shaved to expose the skin. A scalpel fitted with a No. 10 blade was then used to make a sagittal incision starting between the eyes and ending just behind the ear. This type of incision was done to expose the bregma. Bregma was used as a reference point to locate the correct stereotaxic coordinates that targeted injection sites for M1, S1, and S2. With the use of a Hamilton 5 μ L syringe, Green Fluorescent Beads (Lumafloor Inc.) were injected at the correct stereotaxic coordinates. These Fluorescent beads were recognized as retrograde tracers in the mid-1980s (Katz et al., 1984; Katz and Iarovici, 1990) and are highly resistant to fading and offer long-term labeling. Studies have shown that although this type of fluorescent retrograde

tracer is somewhat difficult to use due to their tendency to clump in the injection pipette, latex beads offer stable fluorescence with minimal diffusion from the injection site, exclusive retrograde travel with minimal entry to undamaged fibers of passage, and are non-toxic to neurons so can be used in long duration experiments (Köbbert et al., 2000; Vercelli et al., 2000; Lanciego and Wouterlood, 2011). In this study a total of 2.5 μ L of Green Fluorescent beads where injected at each target site. To determine the correct location of the target sites for each respective surgery a mouse atlas was used to give the correct coordinates respective of the bregma for each respective surgery. Using Bregma as a starting point and the Paxinos atlas (2012), the Hamilton needle was used to move 1.0 mm posterior to Bregma, 1.5 mm to the right of the midline and the injection was made a depth of 0.5 mm into the brain. For callosal S1 surgeries using the bregma as a starting point, using the stereotaxic apparatus to move 1 mm anterior from Bregma, 3.0 mm to the left of the midline and 1 mm deep into the brain. The S1 injections occurred on the opposite side than the S2 and M1 surgeries. Lastly for S2 surgery the coordinates centered 0.1 mm posterior to Bregma, 3.5 mm lateral of the mouse and 3.0 mm deep. 1.5 μ L of beads where injected followed by a wait 7 minutes then the final 1 μ L was injected 0.1 mm deeper into the respective region. This was to ensure that the Green Fluorescent Beads were able to penetrate the entirety of the target region. After the surgeries where completed, the incisions were then closed with Krazy glue and the subject was placed in a separate cage to recover for three days.

2.4 Diolistics preparation and labeling:

Once the three-day recovery period was completed, which allows adequate time for bead transport, each mouse was then injected with 0.1mL of Euthasol and their brains were removed from their skulls. With the recovered brains then placed in an ice bath of diluted 3% artificial

cerebrospinal fluid (ACSF) that was aerated with carbogen (95% O₂ and 5% CO₂). The ACSF that was used to for each respective dissection was composed of 124 mM NaCl, 1mM NaH₂PO₄, 2.2 mM KCl, 2mM CaCl₂, and 2mM MgSO₄. The extracted brain was then placed into a vibratome (Leica Vt 1000s), which cut the coronal brain slices, with the cerebrum facing the blade, at 300 μm in ice cold artificial cerebral spinal fluid (ACSF). The brain slices were then placed into another glass container separate from the initial glass container, containing an aerated ACSF bath. Once the brain was fully sliced, the brain slices where placed into wells which contained more ACSF.

All the collected slices were then put through diolistics and exposed to DiI-coated tungsten particles in helium powered chamber, capable of delivering the dye crystals into the brain slices. This Dye can also be injected in large quantities into the mouse brain. DiI is a lipophilic or fat-loving dye thus it was a perfect secondary tracer for this experiment since it does not influence the overall function of the neuron. Furthermore, diolistics was used to insert the DiI crystals into the brain slices using a helium pressure chamber (Saleeba 2019). The dye crystals were prepared through the dilution of 1.5 mg of 1,1'-Diocadecyl-3,3',3',3'-tetramethylindocarbocyanine iodide (DiI; Invitrogen) in 50 μL methylene chloride. 12.5 mg of tungsten particles which were spread across a glass slide. The dye solution was then used to coat the tungsten particles, once completely coated they were air dried in a temperature-controlled room. Once completely dried, the coated particles were then placed in a 5mL conical tube containing 3ml of distilled water. The conical cube was placed in a sonicator for 20 minutes then three drops of the suspension was transferred to a macrocarrier and allowed to dry at a temperature of 4 °C protected from light using aluminum foil. Each brain slice was exposed to

the macrocarriers using an 1100 PSI rupture disk as its pressure threshold. After labeling was completed, each brain slice was placed back into its respective ACSF-filled well.

2.5 Tissue fixation and storage:

Following diolistics of the brain slices using DiI coated tungsten beads, all sections were fixed with 4% paraformaldehyde dissolved in PBS with a pH 7.4 and stored at a temperature of 4 °C. At this point, the brain slices contain neurons retrogradely labeled by the green beads and from the DiI coated tungsten beads making the brain cells potentially double-labeled. The wells that contained the double labeled slices was wrapped with parafilm to ensure a tight seal of the wells and finally covered completely with aluminum foil to limit light exposure, with the purpose of preventing bleaching of the slices. After two days, all fixed sections then were rinsed three times with a 0.1M phosphate buffer and re-wrapped in parafilm and aluminum foil.

2.6 Imaging:

Brain slices were placed on a slide then cover slipped using vectashield then once dried, the slide was imaged using a confocal microscope operating on an Olympus' Fluoview Imaging System. An initial 10x objective lens (numerical aperture (NA) = 0.40) was used to locate and identify labeled neurons in the S1BF. Imaging was focused on layers 2/3 of the barrel cortex that were double labeled with both green fluorescent beads and DiI tungsten particles. The confocal filters that were used was FitC for the detection of the green fluorescent dye. Its excitation laser wavelength which gave the green emission color was 488nm. The fluorochrome excitation with the multiphoton IR laser for FitC which held with the sharpness of the emission of green was at a wavelength of 750-800nm. The confocal filter used for DiI with a red emission excitation

wavelength being 830-920nm. The criteria for a 'good' neuronal cell was that it must be stained with both dyes for it to be recorded as a double-labeled cell and further used in the reconstruction. Neurons that were double labeled under the 10x objective lens were collected as X-Y-Z-stack images in 1.0 μ m increments through a two-channel acquisition sequentially.

2.7 Reconstruction and Measurements:

Neuronal cell images stacks that were deemed as 'good' during imaging were then transferred to another computer and were three-dimensionally reconstructed with the computer program Neuroleucida (MBF Biosciences Inc.), that allowed for tracing each portion of the selected cell as precisely as possible. The goal of the tracings was to identify the morphological characteristics between the neurons that projected to M1, S1, or S2. The reconstructions of these cells were then analyzed in NeuroExplorer (MBF Biosciences) to obtain the morphometrics of each neuron, the individuals completing the tracings were not blinded to the condition.

2.8 Statistical Analyses:

NeuroExplorer selected the main components needed to run through statistical testing. The component for the cell body include perimeter, area, feret maximum, feret minimum, aspect ratio, compactness, convexity, form factor, roundness, and solidity (see Table 2). Feret min/max is a measure of the largest and smallest diameters of the reconstruction contour. Aspect ratio will indicate the degree of flatness in the soma. Compactness is another method to describe the relationship between the area of the soma and the maximum diameter of the cell body further indicating if the cell shape is circular. Convexity depicts whether the soma is convex or concave in its morphology. Form factor considers the perimeter in its calculations of the soma in order to have a more precise measurement of the overall cell body. Lastly solidity is related to convexity

through its calculations, however, a reconstruction contour can have a decreased value of convexity with an increase of solidity. This is because convexity and solidity are inversely proportional (also see figure 7). The variables that were looked at for the dendrites of the neuronal cells included qty, nodes, ends, length, mean length and lastly complexity which looks at the contours of the dendrites and soma and observes whether they do not have ridges and are smooth (i.e., circles, ellipses) are assigned a value of 1 (Table3). The components that were selected for, account for the morphology of the cell body and the morphology of the dendrites for both the trimmed condition as well as for the non-trimmed condition. Therefore, the component of measures another physical property of the entire neuronal cell. Normally distributed data were described by their mean \pm SEM and SD for each of the experimental conditions and were calculated using NeuroExplorer Program. The statistical tool used to determine significance was done with Statistica (StatSoft). A factorial ANOVA was done to determine significance between the trim and control groups, and projection region of these pyramidal neurons. A post-hoc Tukey HSD test was utilized to find the sources of the statistically significant results.

Chapter 3

Results

3.1 Neuronal Reconstructions:

One hundred and twenty-three double-labeled neurons were collected and distributed into six groups based on the projection target of their axons. Of this total number of collected cells, control, or non-sensory deprived condition of this experiment there were 29 M1 projecting cell, 18 S1-callosal projecting neurons and 16 S2 projecting cells. For the experimental condition or sensory deprived condition there was, 13 M1-projecting cells, 13 S1 projecting cells and 34 S2 projecting cells (Table 1).

Layer 2/3 has a diverse range of neuronal cells; previous research done in the laboratory, has shown that M1- projecting cells typically have either a stellate soma shape with long dendrites or a traditional pyramidal cell shape(Chen et al., 2012; Palaguachi et al.,2017). S1 callosal -projecting cells typically have elongated oblong soma bodies and lastly S2-projecting cells have a more spherical cell body with long dendrites (Figure 5). When comparing sensory deprived cells in Figure 6? and callosal projecting cells in Figure 6, the morphology of the different neuronal phenotypes were dramatically impacted by sensory deprivation. Figure 6A, shows the M1 neurons deprived of their normal sensory inputs via whisker trimming, have a more spherical cell body, with shorter dendritic length than in M1 control cells (Figure 5A). Figure 6B shows the S1 pyramidal cells following sensory deprivation had more triangular shaped somas with longer dendrites than in control conditions (Figure 5B). Lastly, Figure 6C shows S2-projecting cells had an elongated oblong triangle soma with fewer dendrites that were longer following sensory deprivation as compared to control S2 projecting cells in Figure 12C.

In sum, sensory deprivation via whisker trimming of CD-1 mice has resulted in morphological changes and with the gender of the CD-1 mice not making a difference in the results.

3.2 Cell Body:

The neuronal cell body and dendrites have distinct morphology that can be detected using dyes then further analyzed through cellular reconstructions of the cell body and associated dendrites. The most abundant type of neuronal cell in the cerebral cortex are pyramidal cells (Defelipe and Farinas 1992). Focusing in layers 2/3 in the barrel cortex of rodents, the soma, dendrites, and dendrite trees were defined in a baseline/control conditions then further compared to neurons taken from a sensory deprived cortices (see methods).

3.2.1 Perimeter:

The soma perimeter is a representation of length of the reconstructed contour which encircles the cell body. The average perimeter between the three cell groups of the control group showed no statistical difference. M1 projecting cells exhibited an average perimeter of $59.00 \pm 2.96\mu\text{m}$. The baseline perimeter of S1 projecting cells was $58.00 \pm 3.76\mu\text{m}$ and lastly the baseline perimeter of S2 projecting cells was $58 \pm 3.99\mu\text{m}$. After a month of whisker trimming, the cell body size in all three cell types decreased considerably. The average perimeter of a M1 projecting soma was $33 \pm 4.8 \mu\text{m}$, the average perimeter of an S1 sensory deprived cells was $37 \pm 4.4\mu\text{m}$. Lastly the average S2 sensory deprived projecting cell had a perimeter of $42 \pm 2.8\mu\text{m}$. An ANOVA was used to show significance of the sensory deprived and control groups, showing that the condition a cell was in, sensory deprived or control, did have an impact on its perimeter [F (1,113) =40.33, $p < 0.0$]. However, there were no differences between cell type within the two conditions (control or sensory deprived) [F (2,113) =0.54 $p > 0.58$]. The average

percent decrease between the control and sensory deprived projecting cells was 35.44%. Looking at the M1-sensory deprived projecting cells, they have a much smaller perimeter than the control M1 cells, with a percent decrease of 43.31%. S1 and S2 sensory deprived cells also exhibit the same trends, S1 sensory deprived projecting cells exhibited a 35.65% decrease in soma perimeter. S2 sensory deprived projecting cells displayed a 27.37% decrease in soma perimeter. This can be visualized in Figure 8A and directly observed in Table 2. To take this analysis further, a post-hoc Tukey HSD revealed that there are noted differences in the perimeter between the specific cell bodies. For example, M1 control projecting cells had a significant difference in perimeter compared to the M1 sensory deprived projecting cells with a $p < 0.0007$. The same can be seen in S1 control and S1 sensory deprived soma perimeter, S1 control projecting cells are larger than S1 sensory deprived projecting cells ($p < 0.006$). Lastly, S2 control with S2 sensory deprived soma perimeter was also found to have a statistically significant difference ($p < 0.02$). Thus, this demonstrates that trimming whiskers decreases the perimeter of the soma in the S1BF1 region of the mouse brain.

3.2.2 Area:

The area of the soma is calculated at the largest two-dimensional cross-sectional areas that were observed within the boundary of the cell body itself in the x-y-z image stacks. The soma area of the sensory deprived neuronal cells can also be seen to have a significant difference between themselves and the control group [$F(1,113) = 26.4, p < 0.001$]. Figure 8B reveals the observed mean area of the somas of M1 projecting control cells have a larger average area of ($263 \pm 23.5 \mu\text{m}^2$), while M1 sensory deprived projecting cells have a significantly smaller area average of $93 \pm 38.2 \mu\text{m}^2$ (Tukey HSD, $p < 0.003$). S1 callosal cells exhibited an average area of $225 \pm 29.8 \mu\text{m}^2$ while S1 sensory deprived projecting cells also had a slightly smaller average

somal area of $107 \pm 35.1 \mu\text{m}^2$, this difference was not statistically significant $p > 0.11$. Lastly, S2 projecting neurons ($234 \pm 31.7 \mu\text{m}^2$) were indistinguishable from S2 sensory deprived projecting cells even though they did exhibit a smaller average area as well $134 \pm 22.4 \mu\text{m}^2$ this difference was found to not be significant $p > 0.12$. These data show a consistent trend in the somal area between the three control groups relative to the sensory deprived somata: the control groups for all three cell types are much larger than the sensory deprived cells; these differences did not reach statistical significance [$F(2, 113) = 0.71, p > 0.49$].

As seen in Figure 8B, this substantial difference between the control and sensory deprived groups indicate that there is a reduction in the area found in the somata located in supragranular layers of the barrel cortex. The other difference in soma area revealed by the Tukey HSD test, did find a statistical difference between the M1 control projecting cells and S1 sensory deprived cells, with $p < 0.004$. M1 control projecting cells were also found to have a difference with S2 sensory deprived projecting cells with a p value less than 0.05. No other noted differences between the soma bodies were found for S1 or S2 cells.

3.2.3 Soma Roundness and Form Factor:

Similar results are also found in the soma roundness. The soma roundness was computed with circular cells having values close to 1 and elongated cells would have values closer to zero. Neurons from sensory deprived cortices were more elongated than the control groups who were more spherical in shape. M1-projecting cells sensory deprived cells had an average roundness of 0.52 ± 0.03 while control M1 projecting cells had a slightly smaller [higher?] value of 0.66 ± 0.24 . S1 projecting cells in sensory deprived animals have an average of 0.54 ± 0.35 , while S1-projecting cells in the control animals had a slightly rounder mean of 0.60 ± 0.030 . Lastly S2-projecting cells in sensory deprived animals had soma roundness of 0.58 ± 0.02 , whereas the

control group has a rounder soma that averaged 0.63 ± 0.03 . Figure 8C shows these differences as well, exhibiting control soma roundness closer to the value of 1 than in the trim, thus representing that the control cells are larger and rounder than the sensory deprived projecting cells. Furthermore, indicating that the sensory deprived group had a statistically significant more elongated soma than the control groups [F (1,113) =6.9, $p < 0.009$]. Once again there was no difference within groups [Control: F (2,113) =0.94 $p > 0.39$; Sensory Deprived: F (2, 113) =0.618, $p > 0.54$]. No other differences were found between the individual M1, S1, S2 control versus sensory deprived cells were found when conducting a post-hoc test.

Form factor considers the perimeter of the soma ranging from 0 to 1. A value closer to 1 indicates that the soma is more circular while a value of zero leads to a flatter cell body measurement. As seen in the three control groups in Figure 9A, their values are slightly closer to 1 than their sensory deprived counterparts, which have values slightly closer to zero. M1 control projecting cells had an average form factor of 0.84 ± 0.017 , S1 control projecting cells had an average form factor of 0.89 ± 0.022 , S2 control projecting cells had an average form factor of 0.83 ± 0.024 . Sensory deprived M1 projecting cells displayed an average form factor of 0.79 ± 0.029 , S1 projecting cells showed an average form factor of 0.78 ± 0.026 . Lastly sensory deprived S2 projecting cells had an average form factor of 0.80 ± 0.017 . Although there is a slight difference in the sizes of the somata for form factor, there was no statistical significance for comparisons within groups or across conditions (ANOVAs $p > 0.05$). No differences were found for form factor between the individual M1, S1, S2 control vs. sensory deprived cells.

3.2.3 Convexity:

Convexity is a measurement of the cell body profile, measuring if the cell body's shape is convex or concave. Concave observed shape will have a value less than 1. Control M1 projecting

cells had a mean convexity of 0.988 ± 0.0038 , S1 projecting cells had a mean convexity of 0.989 ± 0.0049 . Lastly S2 projecting cells had a mean convexity of 0.985 ± 0.0052 . M1 sensory deprived projecting cells had a mean convexity of 0.990 ± 0.0062 , S1 sensory deprived projecting cells had a mean convexity of 0.990 ± 0.0057 . Lastly, S2 sensory deprived projecting cells had a mean convexity of 0.982 ± 0.003 . There was slight difference in values for convexity between the projecting cells from the control and sensory deprived conditions, these differences were not statistically significant (ANOVAs, $p's > 0.5$). Both groups have convex shapes for their soma (Figure 9D). Convexity differences were not found between the individual M1, S1, S2 control projecting animals versus in either the control or sensory deprived groups.

3.2.4 Solidity and Compactness:

Solidity is inversely related to convexity and proportional to area. The solidity of a reconstructed neuronal body is calculated through the area of the contour divided by the convex area, resulting in a value that ranges from 0-1. Solidity values of 1 indicate a soma shape that is more circular or spherical. Solidity from the control neuronal cells indicate that there is not a significant difference or ($p's > 0.05$) from it and the sensory deprived neuronal cells. M1 control projecting cells had a mean solidity of 0.97 ± 0.0052 with a slight difference between their M1 sensory deprived projecting counter parts, having a solidity value of 0.89 ± 0.0084 . Figure 9B illustrates the M1 sensory deprived projecting cells, have a slightly less solidity circular cell body shape than M1 control projecting cells however, this difference is not enough to be statistically significant. S1 control projecting cells had a solidity value of 0.96 ± 0.006 , with no difference in S1 sensory deprived cells exhibiting the same solidity value of 0.96 ± 0.0077 . Lastly, S2 control projecting cells, revealed that there was a slight difference in the solidity

values compared with the S2 sensory deprived projecting cells. S2 control projecting cells had a solidity value of 0.96 ± 0.0070 and the S2 sensory deprived projecting cells had a solidity value of 0.93 ± 0.0049 . Although, there is a slight difference between the control and sensory deprived S2 values, it is again not significantly different (Table 2). These results indicate that there was no significant result in solidity between either the control or sensory deprived conditions of the neuronal soma in the 2/3 layers of the barrel cortex in mice [$F(1,113) = 0.1, p < 0.81$]. No further differences were found between the individual M1, S1, S2 control vs. M1, S1, S2 sensory deprived cells in post-hoc tests.

Soma compactness is another form of area in comparison to the maximum diameter of the reconstructed contour. It is used as another metric to observe cell body shape, with values also ranging from 0-1. Figure 9C, depicts the M1 sensory deprived projecting cells, have a slightly less solidity circular cell body shape than M1 control projecting cells however, this difference is not enough to be statistically significant. M1 control projecting cells have a mean compactness of 0.81 ± 0.16 with a slight difference between their M1 sensory deprived projecting counterparts, having a compactness value of 0.68 ± 0.026 . S1 control projecting cells had a compactness value of 0.77 ± 0.020 , with a slight difference in S1 sensory deprived cells exhibiting a compactness value of 0.73 ± 0.024 . Lastly, S2 control projecting cells, revealed that there was a slight difference in the compactness values with the S2 Sensory deprived projecting cells. S2 projecting cells has a compactness value of 0.79 ± 0.021 and the S2 sensory deprived projecting cells has a compactness value of 0.74 ± 0.015 . Although, there is a slight difference between the control and sensory deprived S2 values, it is again not significantly different (Table2). Compactness also found no differences in M1, S1, S2 control vs. sensory deprived cells in a post-hoc test, ($p > 0.05$).

3.2.5 Feret Min and Feret Max:

Feret min and feret max is a display of the dimensions of the reconstructed contour of the neuronal cells. Measuring the feret min from the smallest dimensions of the contour perpendicular to the feret max, while feret max measures the longest diameter of the contour. These two measurements are independent of one another and not necessarily at right angles to each other. According to the Figure 10B, the feret min, there is a clear difference between the control M1, S1, S2 projecting cells and the sensory deprived M1, S1, S2 projecting animals [$F(1,113) = 46.6, p < 0.0002$]. Control M1 projecting cells had a mean feret min of $15.4\mu\text{m} \pm 0.78$, while sensory deprived M1 projecting cells had a significantly smaller feret min of $7.95\mu\text{m} \pm 1.27$ (Tukey HSD, $p < 0.001$). Control S1 projecting cells had a mean feret min of $14.6\mu\text{m} \pm 10$ while S1 sensory deprived had significantly smaller $9.2\mu\text{m} \pm 1.17$ as their average feret min (Tukey HSD, $p < 0.008$). Lastly S2 control cells had a $14.9\mu\text{m} \pm 1.06$ average and a mean of $10.27\mu\text{m} \pm 0.75$ for S2 sensory deprived projecting cells this difference was also statistically significant (Tukey HSD, $p < 0.01$).

For feret max, control projecting cells had much larger dimensions than neurons from the sensory deprived condition. There is a significant difference between the control and sensory deprived conditions [$F(1,113) = 32.7, p < 0.0$] with the control cell bodies having a larger feret max. Control M1 projecting cells had a feret max of $21.5\mu\text{m} \pm 1.10$ while M1 sensory deprived projecting cells had a feret max value of $13.05\mu\text{m} \pm 1.79$ this decrease is statistically significant with $p < 0.004$. S1 control projecting cells had a value of $21.5\mu\text{m} \pm 1.40$ but the sensory deprived S1 projecting cells had a value of $14.39\mu\text{m} \pm 1.65$, this decrease in feret max was found to be

statistically significant $p < 0.015$. Lastly, when observing S2 control projecting cells and S2 sensory deprived projecting cells there was an increase of the feret max from $1.5\mu\text{m} \pm 1.48$ in the control to $16.03\mu\text{m} \pm 1.05$ in sensory deprived S2 projecting cells (Tukey HSD, $p < 0.05$) (Table 2).

3.2.6 Aspect Ratio:

Aspect ratio is the ratio of ferret max divided by ferret min to assess the degree of symmetry of the cell body. A value closer to 1 indicates that the soma would be rounder whilst a value closer to zero would have more of a flatter soma. There is a significant difference between the means of the aspect ratios. The sensory deprived conditions differed from the control condition but this comparison was not found to be statistically different [$F(2, 113) = 1.7, p > 0.18$]. In the control groups, the aspect ratio did not greatly differ between the three projecting groups significantly. M1 projecting cells had aspect ratio mean of 1.40 ± 0.068 , S1 projecting cells exhibited an average aspect ratio of 1.50 ± 0.87 and lastly S2 projecting cells exhibited an average aspect ratio of 1.45 ± 0.92 . However, when compared to the sensory deprived projecting cell counterparts there was a difference in the aspect ratio. M1 sensory deprived projecting cells demonstrate a mean aspect ratio of 1.74 ± 0.11 , S1 sensory deprived projecting cells have a mean aspect ratio of 1.66 ± 0.10 . Lastly S2 projecting cells have a mean aspect ratio of 1.55 ± 0.65 (Table 2). These data show that the sensory deprived cell bodies are slightly rounder than the control group. The control group exhibiting an aspect ratio that makes the control soma relatively flatter (Figure 10A). However, statistically there is only a significance between the M1 control and M1 sensory deprived cells, $p < 0.016$. S1 control and S1 Sensory deprived do not have a statistical difference as is the case between S2 control and S2 trim.

3.3 Neuronal Dendrites:

Neurons receive inputs on to their dendrites (Sergio Luengo-Sanchez 2015). The degree and pattern of dendritic branching defines the range and variety of synaptic inputs that a neuron can process; the size and complexity of dendrites tend to differ depending on the neuron's task (Jan & Jan, 2003). Focusing on the dendritic morphology of layer 2/3 pyramidal cells we quantified their metrics in control and sensory deprived animals to see if there is any form of structural plasticity occurring due to alterations in afferent input.

3.3.1 Dendrite Quantity:

Dendrite quantity (qty) was calculated for the control groups and for the sensory deprived group cells. When comparing the dendritic qty between the control and sensory deprived condition, sensory deprived projecting cells had significantly more dendrites than the control at a p-value of 0.001 for the two conditions $F(1, 113) = 11.22, p < 0.001$. The control data for M1 projecting cells showed a qty mean of 5.6 ± 0.327 , in comparison to the M1 sensory deprived projecting cells that had an increase in dendrite qty to 7.1 ± 0.55 dendrites per cell, this difference was not statistically significant ($p = 0.21$).

Control S1 projecting cells have a dendritic qty mean of 5.01 ± 0.41 while sensory deprived S1 projecting cells have a dendritic qty mean of 4.4 ± 0.48 , which were indistinguishable ($p > 0.99$). Lastly, control S2 projecting cells had a dendritic qty mean of 4.0 ± 0.44 and the S2 sensory deprived cells similar to M1 projecting cells showed an increase of dendrites with a qty mean of 6.1 ± 0.30 ($p < 0.0019$, Figure 11A). Based on dendritic quantity there was a significant difference based on the projection location of the neurons [$F(2, 113) = 9.55, p < 0.0014$]. Post-hoc analysis revealed that M1 control cells and S2 control cells had a significant difference ($p < 0.0001$).

3.3.2 Dendrite Nodes:

Dendritic branch points also known as dendritic nodes was the next metric to be calculated for the control groups and for the sensory deprived group cells. When comparing the dendritic nodes between the control and sensory deprived groups there was a significant difference between the two groups. Figure 11B indicates the control data for M1 projecting cells showing a mean number of nodes of 9.2 ± 1.09 , in comparison to the M1 sensory deprived projecting cells that had a non-statistically significant increase in dendrite nodes 12.4 ± 1.85 ($p > 0.67$). Control S1 projecting cells had on average 9.7 ± 1.38 dendritic nodes while sensory deprived S1 projecting cells had a dendritic node mean of 5.0 ± 1.63 ($p > 0.38$). Lastly control S2 projecting cells had 10.4 ± 1.46 dendritic nodes which decreased following sensory deprivation to 6.4 ± 1.15 ($p > 0.23$). Although when an ANOVA was done, it could detect a significant difference between the two groups [$F(2,113) = 5.25, p < 0.0065$]. The Post-hoc tukey HSD found differences in the dendritic branch points; the detected difference lied between M1 and S1 ($p < 0.038$). There were no other differences found between the control and sensory deprived cell classes.

3.3.3. Dendritic Ends:

In general, neurons can receive signals through their dendrites via synapses. Dendritic ends occur at the end of the dendrite and can indicate the complexity of the neuron, with more ends being seen on more complex neurons. They are located at various points throughout the dendritic tree (Urbanska et al., 2008).

When looking at the dendritic ends between the control and sensory deprived groups, there were no significant differences. Figure 11C illustrates all the projecting cells in their respective groups. Sensory deprivation significantly impacted the number of dendritic ends $F(2,113) = 4.86, p < 0.009$. The control data for M1 projecting cells show dendritic ends mean of

15.03 ± 1.22, in comparison to the M1 sensory deprived projecting cells there was an increase in dendrite ends mean to 19.3±2.09, p>0.49. Control S1 projecting cells have a dendritic end mean of 14.8 ± 1.55 while sensory deprived S1 projecting cells have a decrease in the dendritic end mean of 9.30 ±1.83, p>0.10. Lastly control S2 projecting cells have a dendritic end mean of 14.6± 1.65 but in the S2 sensory deprived cells have a decrease in the dendritic ends mean of 12.45 ±1.15(p>0.88, Table 3).

3.3.4 Dendritic length and Mean length:

Total dendritic length was also measured, this is a measurement of the total length for all branched structures of a neuronal cell-type. In comparing the baseline control group, the dendritic lengths, the observed data show that the dendrites are longer compared to the sensory-deprived condition. In general, following deprivation there was a decrease in total dendritic length [F (1,13) =31.49, p<0.0000001]. Figure 5A represents the control data for M1 projecting cells which had a dendritic length of 1116.8µm ± 90.3, in comparison to the M1 sensory deprived projecting cells that had an increase in dendritic length to 861.1 µm ±153.9 (p>0.70). Control, S1 projecting cells had a dendritic length of 1080.9 µm± 114.7 and sensory deprived S1 projecting cells had a significantly shorter dendritic length of 363.7µm± 135.0 (p<0.0002). Lastly control S2 projecting cells have dendritic lengths of 570.5 µm ±121.7 but in the S2 sensory deprived cells have a decrease in the dendritic lengths of 1219µm ±84.7 (p<0.0004).

Analyzing the mean dendritic length, which calculates the means of the total average length for all branched structures of given neuronal cell-type, it indicated the control group had significantly longer dendrites [F (2,113) =4.66, p<0.011]. The control data for M1 projecting cells showed dendritic mean lengths of 204.5 µm ± 16.23, in comparison to the M1 sensory deprived projecting cells had a decrease in dendritic mean lengths to 116.1 µm ±27.65. Control

S1 projecting cells had a dendritic mean length of $217.9 \mu\text{m} \pm 20.61$ while sensory deprived S1 projecting cells had a dendritic mean length of $85.38 \mu\text{m} \pm 24.25$ which was statistically smaller ($p < .001$). Lastly, control S2 projecting cells had dendritic mean lengths of $319.9 \mu\text{m} \pm 21.86$ but in the S2 sensory deprived cells had a statistically significant decrease in the dendritic mean lengths to $104.48 \mu\text{m} \pm 15.22$ also be seen in Figure 5B ($p < 0.001$).

Overall, the conclusion is that the sensory deprived cells are shorter than the control cells in regard to their dendrites.

3.3.5 Dendritic complexity:

Dendritic complexity index (DCI) was determined from the following equation, $DCI = (\sum \text{branch tip orders} + \# \text{ branch tips}) \times (\text{total dendritic length} / \text{total number of primary dendrites})$ (Pillai et al., 2012). This index was used to calculate dendritic complexity found in the control groups and for the sensory deprived group cells. The dendritic complexity between the control and sensory deprived condition shows there was statistical difference between the groups [$F(1,113) = 8.85, p < 0.003$]. According to Table 3, the control data for M1 projecting cells exhibited an average complexity value of 11880 ± 2336 in comparison to the M1 sensory deprived projecting cells that showed a decrease in average complexity value to 1213.1 ± 3979 . Control S1 projecting cells had an average complexity value of $12,763 \pm 2966$ while sensory deprived S1 projecting cells had an average complexity of 2341.3 ± 3490 . Lastly, control S2 projecting cells had an average complexity value of $14,265.4 \pm 3140$, while S2 sensory deprived cells had an increase of dendrites an average complexity value to $3,560.2 \pm 2190$.

3.4 Dendritic trees:

Dendrites are approximately five to seven in quantity, and they project directly from the soma and branch extensively. Dendrites can be defined based on their relationship to the soma.

They usually form tree-like arborization around the neuron, called dendritic trees (Dharani, 2015). Primary dendrites originate from the soma; secondary dendrites result from a bifurcation of the primary dendrite. Tertiary dendrites are a result from secondary dendrite and so on. The dendrites will continue to bifurcate until they reach the end. We calculated what percentage of the different orders dendrites occur in the control and sensory deprived neurons collected. Figure 13, under control conditions (Figure 13D, E, F) and sensory deprived conditions (Figure 13A, B, C); the number of dendrites and the percentage of each type of dendrite. What is apparent is in response to whisker trimming there are differences in the cell types. ANOVA analysis showed that the primary dendritic tree in either the sensory deprived condition or control condition is statistically significant difference in the first order of the dendritic tree [$F(1,117) = 10.54$, $p < 0.0015$]. In addition, this statistical difference can be seen in cells that project to S1 there is an increase in the percentage of primary dendrites, and in secondary dendrites while there is a decrease in tertiary and quaternary dendrites. The same trend is also noticed for the S2 dendrites. In the motor cortex projecting cells, there is not a big change in the first order and the second order dendrites statistically [$F(2, 117) = 2.87$ $p > 0.060$]. In the tertiary order dendrites or third order, there are less dendrites in the M1 sensory deprived projecting cells than the control for M1 projecting cells while in the quaternary order there is no change at all. The post-hoc further supports this by noting, that within the sensory deprived cell group: M1, S1, S2 were all found to have statistical differences within this specific group [$F(2, 117) = 8.4$ $p > 0.0003$].

It was also found that the sensory deprived cells came out to be smaller than the control cells ($p < 0.05$). The main differences found here was between the S2 control projecting cells and the S2 sensory deprived cells for the third dendritic tree order where S2 sensory deprived cells have smaller dendritic trees. Tertiary order cell differences were found between S1 trim and S1

control. The other pair of differences arises from S2 trim and S2 control. Lastly, quaternary order also finds between group differences with S2 control differing from S2 trim. Lately, there is a difference found between S2 control cell and S1 sensory deprived cell.

In general, dendritic quantity will influence the amount of dendritic branching points and nodes. Figure 14A shows the main trends that follow the sensory deprivation on the number of dendritic nodes. When comparing the dendritic tree nodes within the control and sensory deprived condition for first order there is a statistical difference $F(2, 113) = 3.67, p < 0.028$. It was discovered that the cells have statistical differences from within the group of the sensory deprived cells for the first order, M1, S1 and S2. In addition, there was also significance found when comparing the M1, S1, S2 control projecting cells to the M1, S1, S2 sensory deprived projecting cells in the first order.

The effect of sensory deprivation on the dendritic nodes in cells that project to S1 cells has shown an increase in percentage of primary dendritic nodes found in the sensory deprived condition. However, when conducting a post-hoc test this percent increase of the primary dendritic tree nodes was found to not be significant, $p > 0.49$.

When comparing the dendritic tree nodes within the control and sensory deprived condition in the second order there is a statistical difference within each group and the cell counterparts [$F(2, 113) = 5.13, p < 0.05$]. S1 sensory deprived projecting cells also had no change in the secondary nodes in comparison to the control condition, interestingly there is a statistical significance (tukey HSD, $p < 0.018$). In addition, there is also a decrease in the dendritic nodes for sensory deprived cells for tertiary and quaternary nodes as compared to the S1 control groups found in Figure 14D. A post-hoc test further concluded that there is no main statistical

significance in the differences in the S1 sensory deprived projecting cells when compared to the S1 control cells in the third and fourth order.

Figure 14B, S2 sensory deprived cells exhibited an increase in dendritic nodes in the primary and quaternary orders but these cells experienced a decrease in dendritic nodes in the secondary, tukey HSD, $p < 0.005$. In the tertiary order the statistical analysis did not find significance in cells that belonged to either the sensory deprived group or the control, with $F(1,113) = 6.77$, $p > 0.10$. The tertiary orders found significance among the S2 control condition and S2 sensory deprived condition, aligning with the notion that third order S2 sensory deprived cells have less nodes, $p < 0.05$ (Figure 14E). M1 sensory deprived cells seen in Figure 14C had a decrease in the dendritic nodes in the primary, secondary, and tertiary orders while having an increase in the fourth order of dendritic nodes as compared to their M1 control counterparts (Figure 14F). There was no global effect of sensory deprivation through whisker trimmings for the specific cell type nor for the in-between group in the tertiary order.

3.5 Dendritic tree length:

Sensory deprivation can also be seen in dendritic tree length. Figure 15A shows the main trends that follow the sensory deprivation of dendritic tree length. These values were calculated based off the average length order then converted into a percentage for simpler comparisons between the different dendritic orders for length. The effect of sensory deprivation on the tree length in cells that project to S1 is that there is an increase in mean percentage of primary tree length found in the trimmed condition and in the secondary tree length in comparison to the control condition. In addition, there is also a decrease in the tree length in the tertiary and quaternary nodes as compared to the control groups found in Figure 15D.

Figure 14B, S2 sensory deprived cells exhibit an increase in length in the primary order while experiencing no change in the secondary order. In addition, S2 projecting cells experience a decrease in the tree length for the tertiary and quaternary orders as compared to the S2 control condition (Figure 15E). When comparing the dendritic tree lengths between the control and sensory deprived condition in the first order there was a statistical difference of $F(2, 119) = 3.44$, $p < 0.035$. M1 sensory deprived cells seen in Figure 15C had a decrease in the dendritic tree length in primary, secondary, and third orders following the node trend however there was no increase in the fourth order of dendritic nodes as compared to the M1 control condition (Figure 15F). Furthermore, there was no significance found when comparing within the condition of the groups in the first order.

When comparing the dendritic tree lengths within either the sensory deprived group or the control group for the second order there were no statistical differences $F(2, 119) = 0.26$, $p > 0.76$. However, there was a significant difference between the control group and sensory deprived group in the second order, $F(1, 119) = 20.74$, $p < 0.00001$.

This difference was found in S2 control cells being different from S2 trim cells (Tukey HSD, $p < 0.02$). Other neuronal significant differences were found among the M1 control cells which were found to be statistically different from S1 sensory deprived projecting cells (Tukey HSD, $p < 0.001$). M1 control projecting cells were also found to be different from S2 sensory deprived projecting cells (Tukey HSD, $p < 0.0009$), although this comparison may not be relevant. Overall, this statistical analysis indicates that there was a difference in the second order dendrites between the sensory deprived group and the control group but no difference of the projecting cells within the groups.

Significance in the tertiary order was found within the sensory deprived and control groups [$F(1,119) = 50.02, p < 0.001$]. In addition, the between group analysis found statistical significance when comparing the sensory deprived group to the control group having a value of $F(2,119) = 5.66, p < 0.004$. This between group difference was noted by the Tukey HSD, indicating S1 trim is different from S1 control $p < 0.004$. S2 control differs from S2 trim cells (Tukey HSD, $p < 0.001$). These results indicate that sensory deprivation caused the neuronal cells to adapt for the tertiary order of the dendritic tree length.

When observing the significance in the quaternary order for length, it was found that there was significance found among the sensory deprived projecting cells and control projecting cells, [$F(2,119) = 5.14, p < 0.007$]. Figure 15A and 15D shows a decrease in dendritic tree length for S1 sensory deprived cells compared to S1 control projecting cells in the fourth order. This decrease was found to be statistically significant through the post-hoc, ($p < 0.05$). There was also a decrease in the S2 experimental condition cells finding that S2 sensory deprived projecting cells significantly differ from S2 control projecting cells or ($p < 0.0004$). It was also found that S2 control projecting cells are also different from S1 sensory deprived projecting cells, $p < 0.0008$. This indicates that for the fourth order S1 and S2 sensory deprived cells are shorter in length when compared to their baseline S1 and S2 control cells.

Chapter 4:

Discussion

4.1 Summary:

Utilizing the retrograde tracing fluorescent beads in conjunction with diolistic labeling, we were successful in identifying three main classes of neurons M1-projecting, S2-projecting, and callosal S1-projecting neurons residing in the supragranular layers 2/3 of the barrel cortex. Other studies (Ramos et al., 2008) were also able to place these classes of neurons in the supragranular layers and observing that the labeled neurons have characteristic pyramidal cell morphologies.

We measured the neuronal pyramidal cell morphology through different metrics primarily focusing on the soma and dendrites. We then further investigated how these three distinct classes of neurons are morphologically remodeled following chronic sensory deprivation during development. Observing the effects that whisker trimming had on the morphology of the cells located in layers 2/3 of the barrel cortex, it was found that the soma morphology was impacted. The major result was that following sensory deprivation of M1, S1 and S2 projecting neurons had smaller soma perimeters and area when compared to their control counterparts. It is also important to note that dimensionally the sensory deprived cells are also smaller on both the larger (ferret max) and smaller (ferret min) soma axes. Aspect ratio was the only measurement where it was statistically significant for the comparison between the M1 control projecting cells and sensory deprived M1 projecting cells. In comparison with the S1 and S2 cells of both groups, there was no statistical difference in the aspect ratio. This means that the M1 sensory deprived soma bodies were found to be rounder than the M1 control soma bodies. S1 and S2 control and

sensory deprived conditions both exhibited more symmetrical soma bodies according to the aspect ratio. Furthermore, when it comes to other metrics of measure, such as: roundness, solidity, convexity, form factor and compactness, even though there were minor differences between and within the control and sensory deprived groups, these differences were not statistically significant. This was also found in other studies (Chen et al., 2012; Weinfeld, et al., 2000) although these studies observed sensory deprivation in different layers the overall results of sensory deprivation were consistent with what our results are exhibiting. Overall, sensory deprived projecting cell soma bodies were smaller and less round than callosal cells.

Dendrites from these same neurons also showed a difference between the groups. Looking at callosal cells from other studies found that they had more elaborate and numerous dendritic processes such as having more nodes and longer apical dendrites and basal dendrites (Ramos et al., 2008). The adaptations that were found in the sensory deprived dendrites was that there was a lower quantity of them in the sensory deprived neurons compared to the control cells. This means that the M1, S1, S2 sensory deprived projecting cells had less dendritic quantity than their control counterparts. A further step into testing the plasticity of sensory deprived cells, shows that the sensory deprived dendrites were shorter. Furthermore, when it comes to other metrics of measure, such as dendritic nodes and dendritic ends, there was no statistical significance between the two groups. When comparing the control M1, S1, S2 projecting cells and the and sensory deprived M1, S1, S2 projecting cells the values made no difference in the nodes and ends in the dendrites. Overall, sensory deprived neurons had a higher quantity of dendrites which were shorter than the callosal projecting cells.

Taking it a step further and looking at the dendritic tree data on sensory deprivation effects on neurons in Layer 2/3 of the primary somatosensory cortex. The dendritic tree data

were separated into orders. These orders can be defined as the continuous bifurcations of the dendrites. When comparing quantity, nodes lengths and variations in the dendritic trees, there was a clear trend that these categories followed. In most cases there was always an increase in the number and length of the primary dendrites. For secondary dendrites there was an increase in quantity, length, for S1 and S2 deprived cells while showing a decrease in M1. When comparing these categories in the tertiary dendritic tree order the trend follows a decrease in the M1, S1 and S2 sensory deprived projecting cells, namely for quantity, nodes, and length. Finally, in the fourth order of dendritic trees showed an increase in dendritic tree quantity and nodes for M1 and S2 trimmed cells while a decrease in S1 for nodes. This is also held consistent with other studies which focused on similar regions of the rodent brain(Chen et al., 2012; Lee et al., 2009).

4.2 Interpretation of the data

There have been many studies that have observed the effects of sensory deprivation on the primary somatosensory cortex, however there are fewer studies that study the supragranular projecting cells located in layers 2/3.

Our findings indicate that sensory deprivation leads to changes in morphology of the neurons, and such changes can be observed in somatic shape and size, dendritic branching, and dendritic length. The traditional morphology of the neurons in the primary somatosensory cortex M1 projecting neurons is pyramidal-like cells that have long dendrites. S2 projecting neurons are small stellate cells with spherical somas and short branching dendrites. Lastly, S1-projecting neurons are large stellate cells with long branching dendrites (Elston, 2003). A study done on Layer 6 of the barrel cortex found that there was no significant influence on the cell body of the neurons in that layer after sensory deprivation (Chen et al., 2012) .This does not align with our study, where it was found that the perimeter and area of the somata had a statistically significant

decrease in size following sensory deprivation in layers 2/3. Other studies found that the neurons in the sensory deprived condition were longer where their dendritic components were significantly higher in the animals that experienced chronic sensory deprivation compared to control animals (Chen et al., 2012). This is not what our study found for the dendrites in layers 2/3 where the dendritic quantity and lengths were shorter in the sensory deprived projecting cells than in the baseline cells. This leads us to the conclusion that our experiment on the supragranular layers and the projecting neurons are consistent based on results from similar studies on the impact of sensory deprivation on the dendritic length.

Other studies have suggested that the barrel cortex can adapt to sensory deprivation but it may cause a depression in the function of the processing in the layer 2/3 neurons (Glazewski & Fox, 1996). This depression occurs because of a reduction in the efficiency of excitatory synaptic connection between layers 2/3 and layer 4 (Feldman, 2005; Petersen, 2007). This aligns with the findings of my study, in which sensory deprivation caused an anatomical rearrangement of M1, S1, and S2 neuronal cells in layers 2/3, indicating re-organization of the primary somatosensory cortex. A possible consequence of this are altered connections with layer 4 since this layer needs to interact with layer 2/3 for proper signaling of sensory input. This line of thinking aligns with what was found in the results where the M1 sensory deprived cells, have a more spherical soma, with shorter dendrites length than the M1 control cells. S1 sensory deprived cells have a more triangular shaped cell body with longer dendrites than in the S1 control condition. Lastly, S2 cells seem to have adapted to an elongated oblong triangle cell body with fewer dendrites that are longer than in the control S2 cells. These altered neuronal dendrites lengths can affect the transmitted signals between the layers (Schaefer et al., 2003). Since whisker trimming did have an impact on the lengths of the neurons, it can be possible that the signals may not transmit

efficiently leading to less information being processed by the animal when it is exploring its environment due to these morphological changes.

Given that the primary motor projecting cells have changed in their morphology due to sensory deprivation it is possible that motor planning could be impacted as a consequence. The same can be said for the S1 and S2 cells, the morphologies of these cells have been altered due to neonatal whisker trimming. This can cause a lowered instance of sensory information being properly integrated in the primary somatosensory cortex and may also alter the neurons' firing patterns. A study has shown that the morphological changes in these projecting cells are a direct response from whisker- trimming and they can affect the afferent signals that are being directed to layers 2/3(Hardingham et al., 2011). Some morphological changes that (Hardingham et al., 2011) found included the lengths of the dendrites being shorter, and not reaching through the appropriate layers which can have another possible consequence of sensory deprivation as an increase of the probability of cells having lower horizontal complexity in order to have long term potentiation (Hardingham et al., 2011). This further alludes to the point that whisker trimming greatly affects the primary somatosensory cortex and its supragranular cells and their overall function.

These are some of the visual aspects that can be seen in the morphology of the different class cell types through the contours drawn using NeuroLucida (also see figure 5 and 6 for full comparison).

4.3 Limitations of the study:

The main limitations of the study can be attributed to the method of staining. Diolistics was used to shoot DiI tungsten particles into the collected brain slices. The reason this method of labeling neurons was a limitation since this method does not evenly cover the brain slices thus some areas of the brain were oversaturated, and other areas were undersaturated. This limited data collection of the neuronal cells as well as their reconstruction and further analysis. This method of staining also does not stain neuronal axons; therefore, data collection of the axons is not possible. Another limitation was the Hamilton needles used to inject the green bead dye into the brain during surgery. Its use significantly inhibited its capability of injecting the green beads due to the needle easily clogging and its difficulty to clean after surgeries. These methods of administering both dyes to the mouse brains limit the capacity to collect double-labeled cells. As an alternative, transgenic mice which already have green fluorescent protein (GFP), and using immunohistochemistry for the detection of the neurons could be used as a substitute for diolistics and the green fluorescent beads in order to find neurons in the S1BF1 region of the barrel cortex. A final limitation is that the investigator was not blinded to the condition, but given the magnitude of the effects and previous research showing dendritic and somatic changes following whisker trimming (Chen et al. 2012), this is likely not a crucial issue. We did not specifically characterize gender's impact on morphology, but based on our and previous data (Chen et al. 2012) using this same paradigm we do not believe this is a significant contributor to our results.

Future studies may expand on this current data set by through the introduction of sensory enrichment. The current data can be used as a baseline for a comparison to the introduction of stimulating mice with trimmed whiskers. These studies can focus on the full effects of sensory deprivation and sensory enrichment and its effects on the morphology of the supragranular

projecting neurons. Other studies have demonstrated that mice will move their whiskers during explorations. These explorations though are weak sensory response they are still evoked by passive stimuli. Whisker-related sensory processing is important for these animal subjects (Petersen 2007). Thus, the exploration of trimmed sensory excitation can be` the next step in a future direction of this study

Figure Legends:

Figure 1: (A) Signaling pathway from whisker to cortex. From S1 the sensory signals are further distributed to other brain areas, including primary motor cortex (M1). Whisker M1 projects to the brain stem, where it contributes to controlling active whisker movement. (B) The whiskers emerge from follicles arranged in a highly stereotypical pattern on the snout of the mouse. The C2 whisker follicle is highlighted in yellow. The S1 barrel cortex contains a somatotopically arranged array of barrels in layer 4, which are laid out in an almost identical pattern to the whisker follicles on the snout. The C2 barrel is highlighted in yellow. (adapted from Aronoff et al., 2010).

Figure 2: A neuronal cell following diolistics treatment, taken with the use of the program NeuroLucida.

Figure 3: An example of a neuronal cell (A) that contains green fluorescent beads and (B) Labeling due to DiI tungsten crystals (red). (C) shows how this neuronal cell is doubly labeled with both dyes. The neuron is highlighted with a blue arrow in each Figure.

Figure 4: (A) An example of what the collected x-y-z stack look like in the program NeuroLucida. (B) this panel shows how the NeuroLucida program can be used to create the contours of the soma body and dendrites. (C, D) The contours are can be analyzed by NeuroExplorer.

Figure 5 Control neuronal cells: These panels are examples of what the control M1, S1, and S2 cell flattened x-y-z stacks look like in NeuroLucida, included are the contours. (A) M1 cells typically have either a stellate- like soma shape with long dendrites or a traditional pyramidal cell shape. (B) S1 cells typically have elongated oblong soma bodies. (C.) S2 cells have a more spherical soma body with long dendrites. Panels D, E, F show the contours of these neurons.

Figure 6 Sensory deprived cells compared to control cells: (A) M1 cells, have a more spherical soma body, with shorter dendrites length than the M1 control cells. (B) S1 cells in the sensory deprived condition have a more triangular shaped soma body with longer dendrites than in the S1 control condition. (C) Lastly, S2 cells seem to have adapted to an elongated oblong triangle soma body with fewer dendrites that are longer than in the control S2 cells. (D, E, F) These are some of the visual aspects that can be seen in the morphology of the different class cell types through the contours drawn using NeuroLucida.

Figure 7: This chart represents the metrics used in measuring the soma body of each respective neuron. These metrics come from NeuroExplorer program (Adaptation *from:* A.C. Barrientos 2019 SFN poster)

Figure 8: Perimeter, Area, and soma roundness bar graphs for the control and trim

groups: The average values found from the (A) soma perimeter, (B) soma area and (c) and soma roundness for the control and trim groups. The x-axis indicates the type of cell and in the experimental group it belongs to. The Y-axis indicates the variable quantity for a given parameter. Bar graphs illustrate the population means with error bars representing the standard error of the mean.

Figure 9: Form factor, solidity, compactness, convexity: The average values found from the (A) form factor, (B) solidity, (C) compactness, (D) convexity of the soma for the control and trim cell groups. The x-axis indicates the type of cell and in the experimental group it belongs to. The Y-axis indicates the variable quantity for a given parameter. Bar graphs illustrate the population means with error bars representing the standard error of the mean

Figure 10: Aspect ratio, feret min, feret max: The average values found from the (A) aspect ratio, (B) feret min, (C)feret max of the soma for the control and trim groups. The x-axis indicates the type of cell and in the experimental group it belongs to. The Y-axis indicates the variable quantity for a given parameter. Bar graphs illustrate the population means with error bars representing the standard error of the mean.

Figure 11: Dendrite quantity, dendrite nodes, dendrite ends: the average values found for the (A). Dendrite quantity, (B) dendrite nodes, (C) dendrite ends for the dendrites from the control and trim cells. The x-axis indicates the cell and which group it belongs to. The Y-axis describes the values for a given perimeter. Bar graphs each illustrate the population means with error bars representing the standard error of the mean.

Figure 12: length, mean length, dendritic complexity: The average values found for the (A) Dendrite length (B) dendrite mean length and, (C) dendritic complexity for the dendrites from the control and trim cells. The x-axis indicates the cell and which group it belongs to. The Y-axis describes the values for a given perimeter. Bar graphs each illustrate the population means with error bars representing the standard error of the mean.

Figure 13: Tree Quantity: Depicts the quantity of dendritic trees there are in each order. Pie charts represents data in percent form and for the control and trim cell groups. Panels A and D shows the percent differences in dendritic tree orders for S1 cell in the control and sensory deprived groups. Panels B and E shows the percent differences in dendritic tree orders for S2 cell in the control and sensory deprived groups. Panel C and F shows the percent differences in dendritic tree orders for M1 cell in the control and sensory deprived groups.

Figure 14 Tree Nodes: Depicts the tree nodes of dendritic trees there are in each order. Pie charts represent data in percent form and for the control and trim cell groups. Depicts the nodes of dendritic trees there are in each order. Pie charts represents data in percent form and for the control and trim cell groups. Panels A and D shows the percent differences in dendritic tree orders for S1 cell in the control and sensory deprived groups. Panels B and E shows the percent differences in dendritic tree orders for S2 cell in the control and sensory deprived groups. Panel C and F shows the percent differences in dendritic tree orders for M1 cell in the control and sensory deprived groups.

Figure 15 Total length: Depicts the tree length of dendritic trees there are in each order. Pie charts represent data in percent form and for the control and trim cell groups. Depicts the quantity of dendritic trees there are in each order. Pie charts represents data in percent form and for the control and trim cell groups. Panels A and D shows the percent differences in dendritic tree orders for S1 cell in the control and sensory deprived groups. Panels B and E shows the percent differences in dendritic tree orders for S2 cell in the control and sensory deprived groups. Panel C and F shows the percent differences in dendritic tree orders for M1 cell in the control and sensory deprived groups.

Table Legends

Table 1 Neuronal population: the total number of cells used in the entirety of the experiment. categorized by cell type and experimental condition.

Table 2 Group means of soma body measurements: Parameters of the soma body, perimeter, area, feret max, feret min, aspect ratio, complexity, convexity, solidity, compactness, form factor and roundness.

Table 3 Dendritic group means: Parameters of the dendrite for the trim and control cells. Focused on the metrics of quality, nodes, length, mean length, and complexity of the dendrites.

References

- Aghion, D. M., & Rees Cosgrove, G. (2014). *Chapter 5 - Surgical Interventions for Pain* (C. Y. B. T.-C. P. and B. A. Saab (ed.); pp. 75–93). Academic Press.
<https://doi.org/https://doi.org/10.1016/B978-0-12-398389-3.00005-4>
- Albieri, G., Barnes, S. J., de Celis Alonso, B., Cheetham, C. E. J., Edwards, C. E., Lowe, A. S., Karunaratne, H., Dear, J. P., Lee, K. C., & Finnerty, G. T. (2015). Rapid Bidirectional Reorganization of Cortical Microcircuits. *Cerebral Cortex (New York, N.Y. : 1991)*, *25*(9), 3025–3035. <https://doi.org/10.1093/cercor/bhu098>
- Alexander, A. S., & Hasselmo, M. E. (2018). Shedding light on stellate cells. *ELife*, *7*.
<https://doi.org/10.7554/eLife.41041>
- Allen, C. B., Celikel, T., & Feldman, D. E. (2003). Long-term depression induced by sensory deprivation during cortical map plasticity in vivo. *Nature Neuroscience*, *6*(3), 291–299.
<https://doi.org/10.1038/nn1012>
- Alloway, K. D. (2007). Information Processing Streams in Rodent Barrel Cortex: The Differential Functions of Barrel and Septal Circuits. *Cerebral Cortex*, *18*(5), 979–989.
<https://doi.org/10.1093/cercor/bhm138>
- Alloway, K. D., Zhang, M., & Chakrabarti, S. (2004). Septal columns in rodent barrel cortex: Functional circuits for modulating whisking behavior. *Journal of Comparative Neurology*, *480*(3), 299–309. <https://doi.org/10.1002/cne.20339>
- Chen, C.-C., Bajnath, A., & Brumberg, J. C. (2014). The Impact of Development and Sensory Deprivation on Dendritic Protrusions in the Mouse Barrel Cortex. *Cerebral Cortex*, *25*(6), 1638–1653. <https://doi.org/10.1093/cercor/bht415>
- Chen, C.-C., Tam, D., & Brumberg, J. C. (2012). Sensory deprivation differentially impacts the dendritic development of pyramidal versus non-pyramidal neurons in layer 6 of mouse barrel cortex. *Brain Structure & Function*, *217*(2), 435–446.
<https://doi.org/10.1007/s00429-011-0342-9>
- Chen, J. L., Voigt, F. F., Javadzadeh, M., Krueppel, R., & Helmchen, F. (2016). Long-range population dynamics of anatomically defined neocortical networks. *ELife*, *5*.
<https://doi.org/10.7554/eLife.14679>
- Daniel E. Feldman, M. B. (2005). Map plasticity in somatosensory cortex. *Science*, *310*(5749), 810–815.
- Dharani, K. (2015). Chapter 1 - Functional Anatomy of the Brain. In K. Dharani (Ed.), *The Biology of Thought* (pp. 3–29). Academic Press.
<https://doi.org/https://doi.org/10.1016/B978-0-12-800900-0.00001-4>
- Diamond, M. E., von Heimendahl, M., Knutsen, P. M., Kleinfeld, D., & Ahissar, E. (2008). “Where” and “what” in the whisker sensorimotor system. *Nature Reviews Neuroscience*, *9*(8), 601–612. <https://doi.org/10.1038/nrn2411>

- Elston, G. N. (2003). Cortex, cognition and the cell: new insights into the pyramidal neuron and prefrontal function. *Cerebral Cortex (New York, N.Y. : 1991)*, *13*(11), 1124–1138. <https://doi.org/10.1093/cercor/bhg093>
- Feldmeyer, D. (2012). Excitatory neuronal connectivity in the barrel cortex . In *Frontiers in Neuroanatomy* (Vol. 6, p. 24). <https://www.frontiersin.org/article/10.3389/fnana.2012.00024>
- Ferezou, I., Haiss, F., Gentet, L. J., Aronoff, R., Weber, B., & Petersen, C. C. H. (2007). Spatiotemporal Dynamics of Cortical Sensorimotor Integration in Behaving Mice. *Neuron*, *56*(5), 907–923. <https://doi.org/10.1016/j.neuron.2007.10.007>
- Fernando Palaguachi, Danna Shimuny, A. E. (2017). *A quantitative morphological analysis of supragranular neurons in the mouse barrel cortex. 1*, 26.
- Friedman, W. A., Zeigler, H. P., & Keller, A. (2012). Vibrissae motor cortex unit activity during whisking. *Journal of Neurophysiology*, *107*(2), 551–563. <https://doi.org/10.1152/jn.01132.2010>
- Gan, W.-B., Grutzendler, J., Wong, W. T., Wong, R. O. L., & Lichtman, J. W. (2000). Multicolor DiOlistic Labeling of the Nervous System Using Lipophilic Dye Combinations. *Neuron*, *27*(2), 219–225. [https://doi.org/10.1016/S0896-6273\(00\)00031-3](https://doi.org/10.1016/S0896-6273(00)00031-3)
- Glazewski, S., & Fox, K. (1996). Time course of experience-dependent synaptic potentiation and depression in barrel cortex of adolescent rats. *Journal of Neurophysiology*, *75*(4), 1714–1729. <https://doi.org/10.1152/jn.1996.75.4.1714>
- Hardingham, N. R., Gould, T., & Fox, K. (2011). Anatomical and sensory experiential determinants of synaptic plasticity in layer 2/3 pyramidal neurons of mouse barrel cortex. *Journal of Comparative Neurology*, *519*(11), 2090–2124. <https://doi.org/10.1002/cne.22583>
- Hardingham, N., Wright, N., Dachtler, J., & Fox, K. (2008). Sensory deprivation unmasks a PKA-dependent synaptic plasticity mechanism that operates in parallel with CaMKII. *Neuron*, *60*(5), 861–874. <https://doi.org/10.1016/j.neuron.2008.10.018>
- Holmgren, C., Harkany, T., Svennenfors, B., & Zilberter, Y. (2003). Pyramidal cell communication within local networks in layer 2/3 of rat neocortex. *The Journal of Physiology*, *551*(Pt 1), 139–153. <https://doi.org/10.1113/jphysiol.2003.044784>
- Inan, M., & Crair, M. C. (2007). Development of Cortical Maps: Perspectives From the Barrel Cortex. *The Neuroscientist*, *13*(1), 49–61. <https://doi.org/10.1177/1073858406296257>
- Ismailov I, Kalikulov D, Inoue T, F. M. 2004. (2004). The kinetic profile of intracellular calcium predicts long-term potentiation and long-term depression. *J Neurosci*, *24*, 9847–9861.
- Jan, Y.-N., & Jan, L. Y. (2003). The Control of Dendrite Development. *Neuron*, *40*(2), 229–242. [https://doi.org/https://doi.org/10.1016/S0896-6273\(03\)00631-7](https://doi.org/https://doi.org/10.1016/S0896-6273(03)00631-7)
- Kaas, J. H. (2000). Organizing Principles of Sensory Representations. In *Evolutionary Developmental Biology of the Cerebral Cortex* (pp. 188–205). <https://doi.org/doi:10.1002/0470846631.ch13>

- Katz, L. C., Burkhalter, A., & Dreyer, W. J. (1984). Fluorescent latex microspheres as a retrograde neuronal marker for in vivo and in vitro studies of visual cortex. *Nature*, *310*(5977), 498–500. <https://doi.org/10.1038/310498a0>
- Kelly, M. K., Carvell, G. E., Kodger, J. M., & Simons, D. J. (1999). Sensory loss by selected whisker removal produces immediate disinhibition in the somatosensory cortex of behaving rats. *The Journal of Neuroscience: The Official Journal of the Society for Neuroscience*, *19*(20), 9117–9125. <https://doi.org/10.1523/JNEUROSCI.19-20-09117.1999>
- Kim, B. G., Dai, H.-N., McAtee, M., Vicini, S., & Bregman, B. S. (2007). Labeling of dendritic spines with the carbocyanine dye DiI for confocal microscopic imaging in lightly fixed cortical slices. *Journal of Neuroscience Methods*, *162*(1–2), 237–243. <https://doi.org/10.1016/j.jneumeth.2007.01.016>
- Lee, L.-J., Chen, W.-J., Chuang, Y.-W., & Wang, Y.-C. (2009). Neonatal whisker trimming causes long-lasting changes in structure and function of the somatosensory system. *Experimental Neurology*, *219*(2), 524–532. <https://doi.org/10.1016/j.expneurol.2009.07.012>
- Li, H., & Crair, M. C. (2011). How do barrels form in somatosensory cortex? *Annals of the New York Academy of Sciences*, *1225*, 119–129. <https://doi.org/10.1111/j.1749-6632.2011.06024.x>
- Lübke, J., Roth, A., Feldmeyer, D., & Sakmann, B. (2003). Morphometric Analysis of the Columnar Innervation Domain of Neurons Connecting Layer 4 and Layer 2/3 of Juvenile Rat Barrel Cortex. *Cerebral Cortex*, *13*(10), 1051–1063. <https://doi.org/10.1093/cercor/13.10.1051>
- Mao, T., Kusefoglou, D., Hooks, B. M., Huber, D., Petreanu, L., & Svoboda, K. (2011). Long-Range Neuronal Circuits Underlying the Interaction between Sensory and Motor Cortex. *Neuron*, *72*(1), 111–123. <https://doi.org/https://doi.org/10.1016/j.neuron.2011.07.029>
- Margolis, D. J., Lütcke, H., Schulz, K., Haiss, F., Weber, B., Kügler, S., Hasan, M. T., & Helmchen, F. (2012). Reorganization of cortical population activity imaged throughout long-term sensory deprivation. *Nature Neuroscience*, *15*(11), 1539–1546. <https://doi.org/10.1038/nn.3240>
- Menzel, R. R., & Barth, D. S. (2005). Multisensory and Secondary Somatosensory Cortex in the Rat. *Cerebral Cortex*, *15*(11), 1690–1696. <https://doi.org/10.1093/cercor/bhi045>
- Metzner, W., & Juranek, J. (1997). A sensory brain map for each behavior? *Proceedings of the National Academy of Sciences*, *94*(26), 14798 LP – 14803. <https://doi.org/10.1073/pnas.94.26.14798>
- Micheva, K. D., & Beaulieu, C. (1995). An anatomical substrate for experience-dependent plasticity of the rat barrel field cortex. *Proceedings of the National Academy of Sciences of the United States of America*, *92*(25), 11834–11838. <https://doi.org/10.1073/pnas.92.25.11834>
- Narayanan, R. T., Egger, R., Johnson, A. S., Mansvelder, H. D., Sakmann, B., de Kock, C. P. J., & Oberlaender, M. (2015). Beyond Columnar Organization: Cell Type- and Target Layer-Specific Principles of Horizontal Axon Projection Patterns in Rat Vibrissal Cortex.

- Cerebral Cortex* (New York, N.Y. : 1991), 25(11), 4450–4468.
<https://doi.org/10.1093/cercor/bhv053>
- Oberlaender, M., Boudewijns, Z. S. R. M., Kleele, T., Mansvelder, H. D., Sakmann, B., & de Kock, C. P. J. (2011). Three-dimensional axon morphologies of individual layer 5 neurons indicate cell type-specific intracortical pathways for whisker motion and touch. *Proceedings of the National Academy of Sciences*, 108(10), 4188 LP – 4193.
<https://doi.org/10.1073/pnas.1100647108>
- Petersen, C. C. H. (2007). The Functional Organization of the Barrel Cortex. *Neuron*, 56(2), 339–355. <https://doi.org/https://doi.org/10.1016/j.neuron.2007.09.017>
- Petersen, C. C. H., & Crochet, S. (2013). Synaptic Computation and Sensory Processing in Neocortical Layer 2/3. *Neuron*, 78(1), 28–48. <https://doi.org/10.1016/j.neuron.2013.03.020>
- Pillai, A. G., de Jong, D., Kanatsou, S., Krugers, H., Knapman, A., Heinzmann, J.-M., Holsboer, F., Landgraf, R., Joëls, M., & Touma, C. (2012). Dendritic morphology of hippocampal and amygdalar neurons in adolescent mice is resilient to genetic differences in stress reactivity. *PLoS One*, 7(6), e38971–e38971. <https://doi.org/10.1371/journal.pone.0038971>
- Ramos, R. L., Tam, D. M., & Brumberg, J. C. (2008). Physiology and morphology of callosal projection neurons in mouse. *Neuroscience*, 153(3), 654–663.
<https://doi.org/10.1016/j.neuroscience.2008.02.069>
- Rocco-Donovan, M., Ramos, R. L., Giraldo, S., & Brumberg, J. C. (2011). Characteristics of synaptic connections between rodent primary somatosensory and motor cortices. *Somatosensory & Motor Research*, 28(3–4), 63–72.
<https://doi.org/10.3109/08990220.2011.606660>
- Sadaka Liza Weinfeld, Edward L. White, Yair, D. L. L. (2000). Effects of sensory deprivation on the development of asymmetrical synapses in mouse barrels. *Somatosensory & Motor Research*, 17(3), 245–254. <https://doi.org/10.1080/08990220050117600>
- Santiago, L. F., Freire, M. A. M., Picanço-Diniz, C. W., Franca, J. G., & Pereira, A. (2019). The Organization and Connections of Second Somatosensory Cortex in the Agouti . In *Frontiers in Neuroanatomy* (Vol. 12, p. 118).
<https://www.frontiersin.org/article/10.3389/fnana.2018.00118>
- Schaefer, A. T., Larkum, M. E., Sakmann, B., & Roth, A. (2003). Coincidence detection in pyramidal neurons is tuned by their dendritic branching pattern. *Journal of Neurophysiology*, 89(6), 3143–3154. <https://doi.org/10.1152/jn.00046.2003>
- Schofield, B. R. (2008). Retrograde axonal tracing with fluorescent markers. *Current Protocols in Neuroscience, Chapter 1*, Unit 1.17. <https://doi.org/10.1002/0471142301.ns0117s43>
- Stern, E. A., Maravall, M., & Svoboda, K. (2001). Rapid Development and Plasticity of Layer 2/3 Maps in Rat Barrel Cortex In Vivo. *Neuron*, 31(2), 305–315.
[https://doi.org/https://doi.org/10.1016/S0896-6273\(01\)00360-9](https://doi.org/https://doi.org/10.1016/S0896-6273(01)00360-9)
- Woolsey, T. A., Welker, C., & Schwartz, R. H. (1975). Comparative anatomical studies of the Sml face cortex with special reference to the occurrence of “barrels” in layer IV. *Journal of Comparative Neurology*, 164(1), 79–94. <https://doi.org/10.1002/cne.901640107>

Zagha, E., Casale, A. E., Sachdev, R. N. S., McGinley, M. J., & McCormick, D. A. (2013). Motor Cortex Feedback Influences Sensory Processing by Modulating Network State. *Neuron*, 79(3), P567-578.

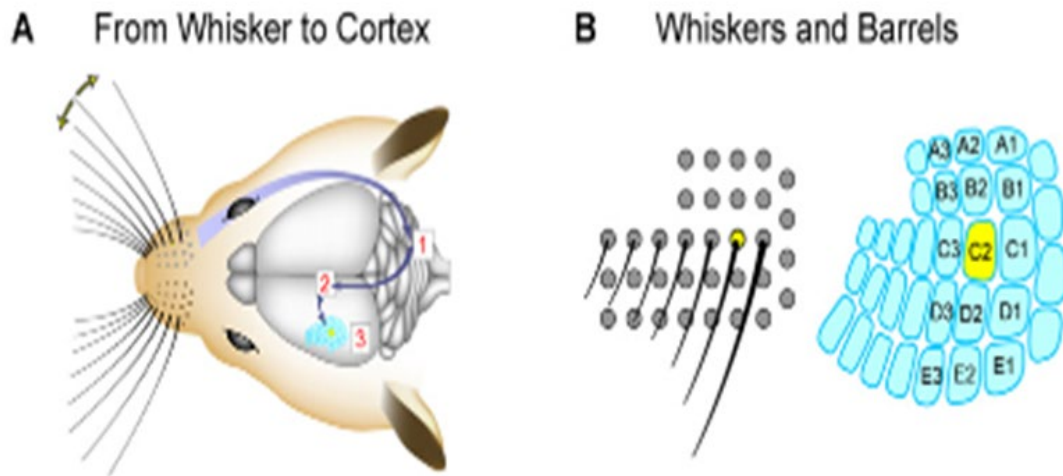


Figure 1: (A) Signaling pathway from whisker to cortex. From S1 the sensory signals are further distributed to other brain areas, including primary motor cortex (M1). Whisker M1 projects to the brain stem, where it contributes to controlling active whisker movement. (B) The whiskers emerge from follicles arranged in a highly stereotypical pattern on the snout of the mouse. The C2 whisker follicle is highlighted in yellow. The S1 barrel cortex contains a somatotopically arranged array of barrels in layer 4, which are laid out in an almost identical pattern to the whisker follicles on the snout. The C2 barrel is highlighted in yellow. (adapted from Aronoff et al., 2010).

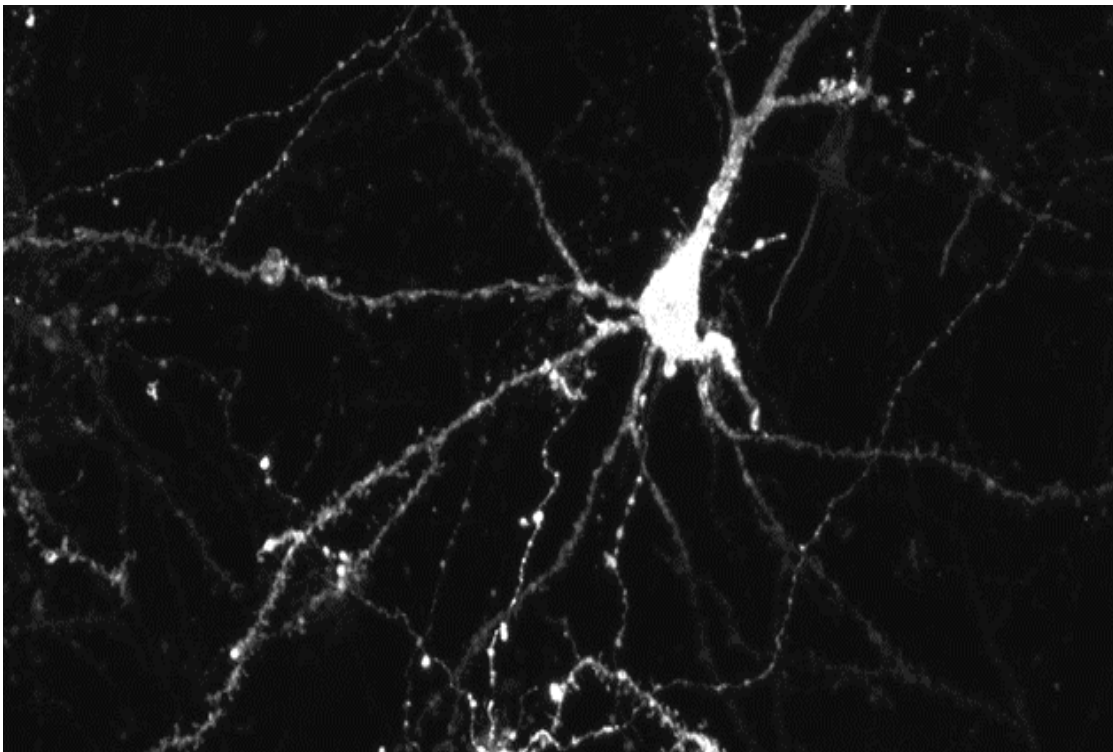


Figure 2: A neuronal cell following diolistics treatment, taken with the use of the program NeuroLucida.

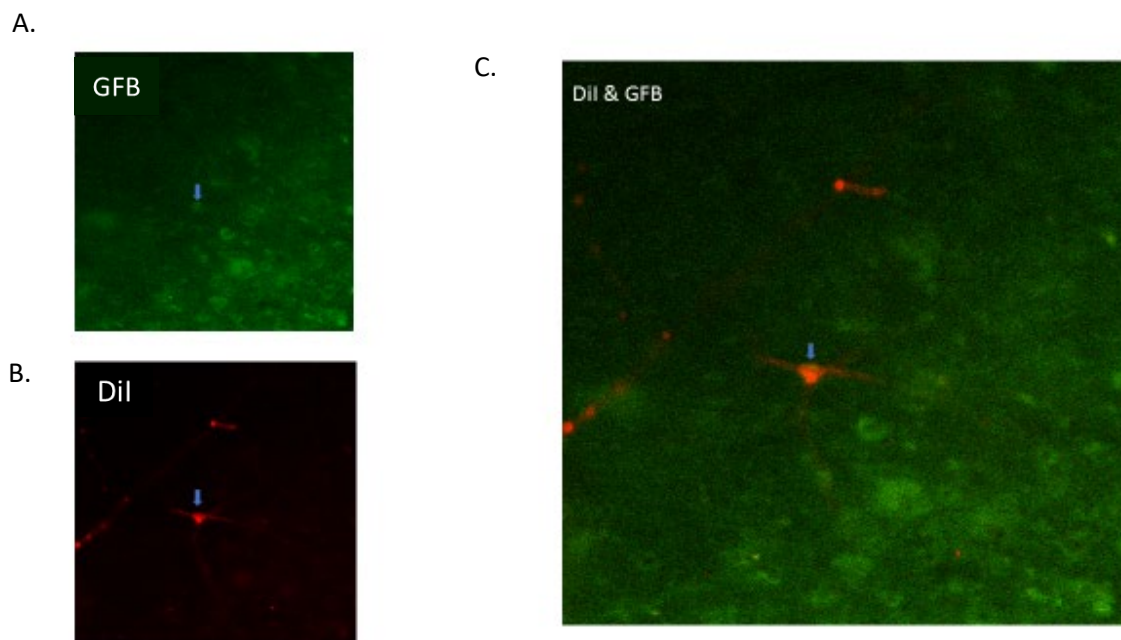


Figure 3: An example of a neuronal cell (A) that contains green fluorescent beads and (B) Labeling due to DiI tungsten crystals (red). (C) shows how this neuronal cell is doubly labeled with both dyes. The neuron is highlighted with a blue arrow in each Figure.

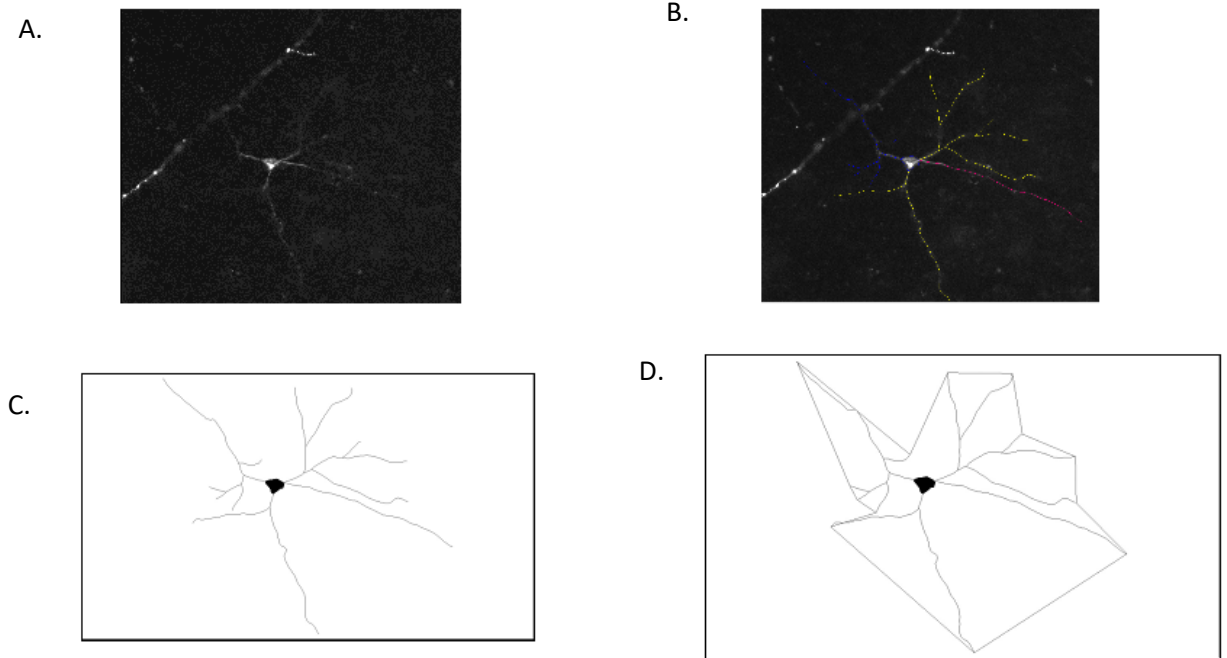


Figure 4: (A) An example of what the collected x-y-z stack look like in the program NeuroLucida. (B) this panel shows how the NeuroLucida program can be used to create the contours of the soma body and dendrites. (C, D) The contours are can be analyzed by NeuroExplorer

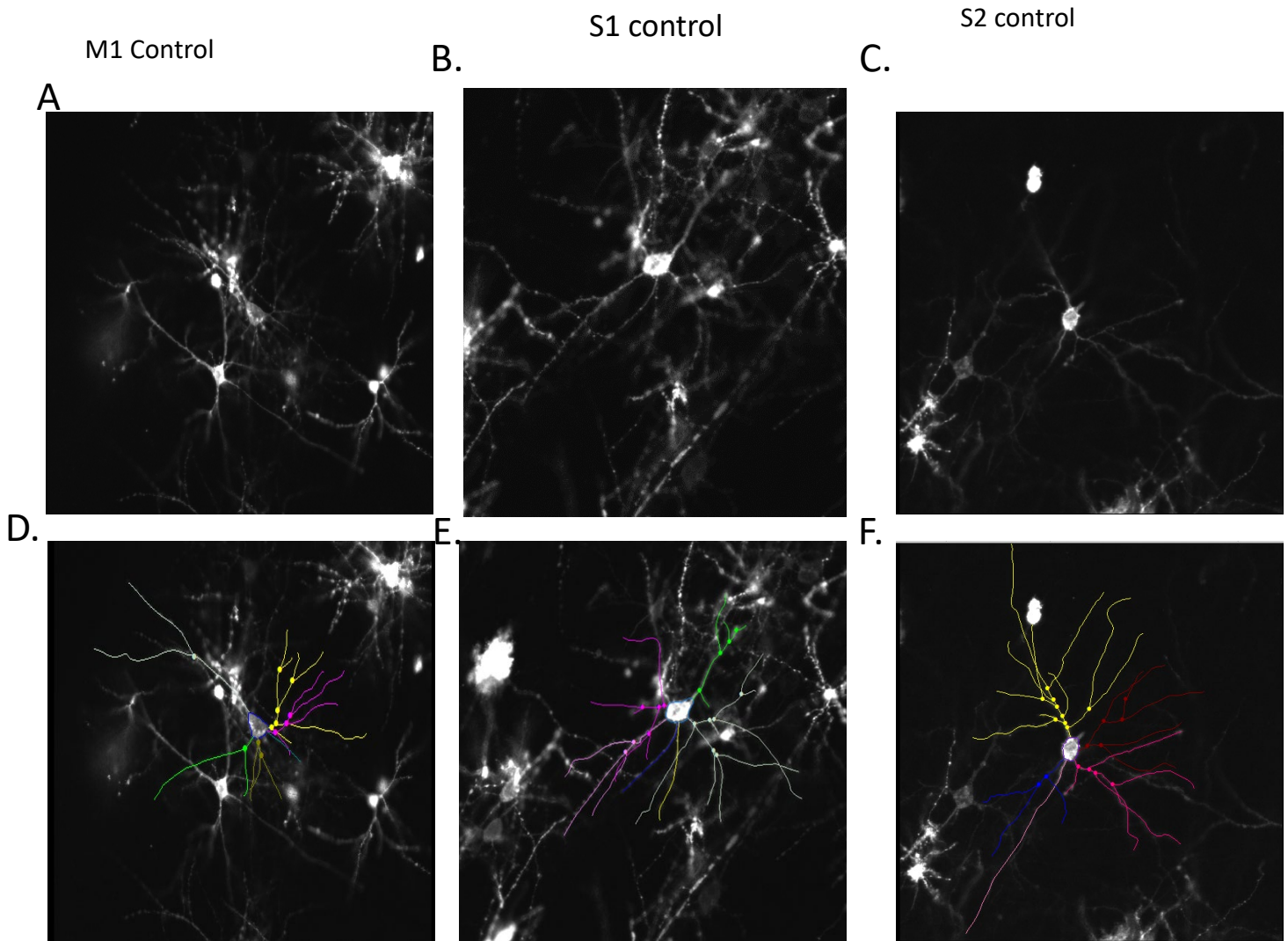


Figure 5 Control neuronal cells: These panels are examples of what the control M1, S1, and S2 cell flattened x-y-z stacks look like in NeuroLucida, included are the contours. (A) M1 cells typically have either a stellate- like soma shape with long dendrites or a traditional pyramidal cell shape. (B) S1 cells typically have elongated oblong soma bodies. (C.) S2 cells have a more spherical soma body with long dendrites. Panels D, E, F show the contours of these neurons

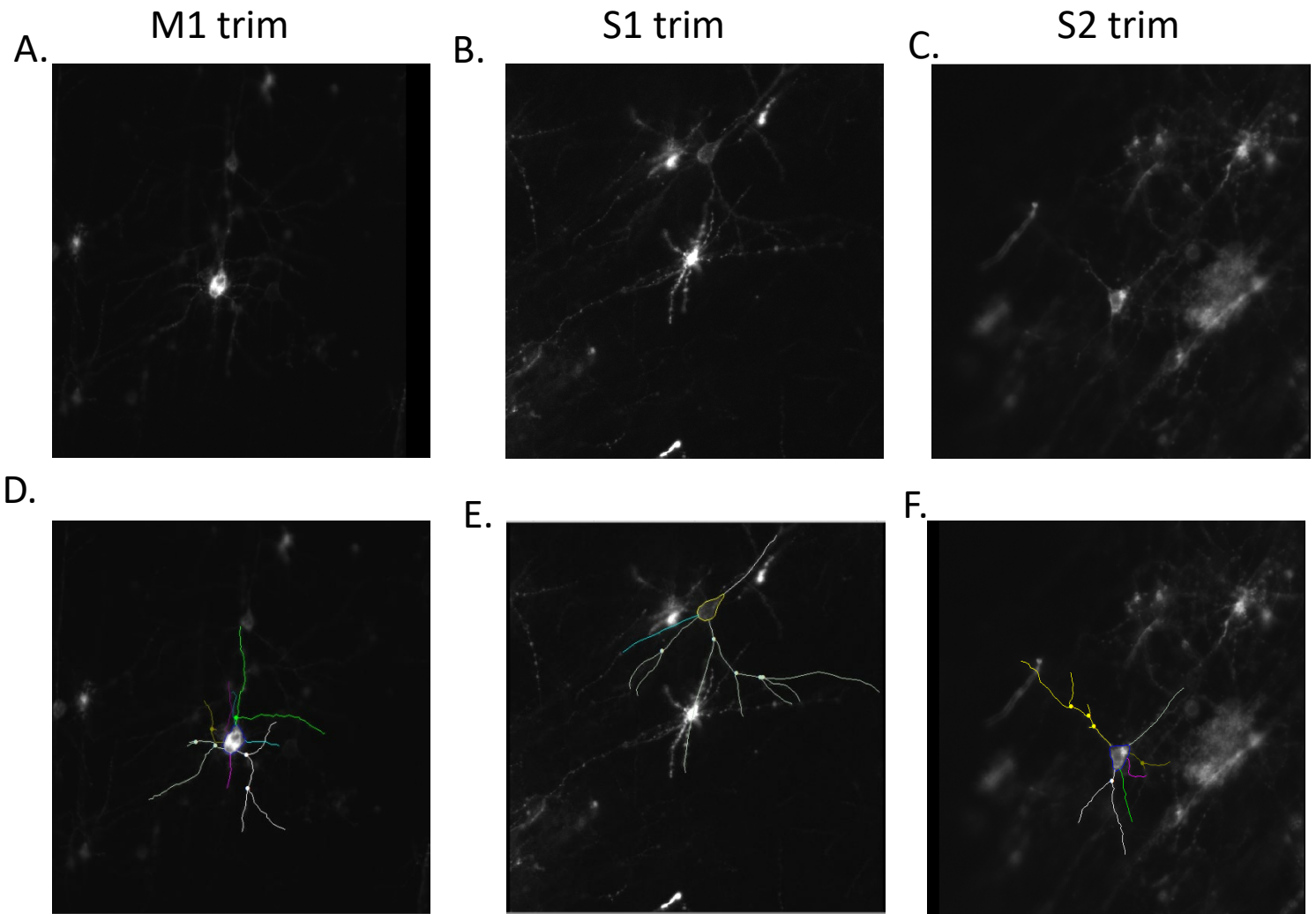


Figure 6 Sensory deprived cells compared to control cells: (A) M1 cells, have a more spherical soma body, with shorter dendrites length than the M1 control cells. (B) S1 cells in the sensory deprived condition have a more triangular shaped soma body with longer dendrites than in the S1 control condition. (C) Lastly, S2 cells seem to have adapted to an elongated oblong triangle soma body with fewer dendrites that are longer than in the control S2 cells. (D, E, F) These are some of the visual aspects that can be seen in the morphology of the different class cell types through the contours drawn using NeuroLucida.

Soma morphology analysis

Using NeuroLucida Explorer (MBF) we conducted the following contour analyses:

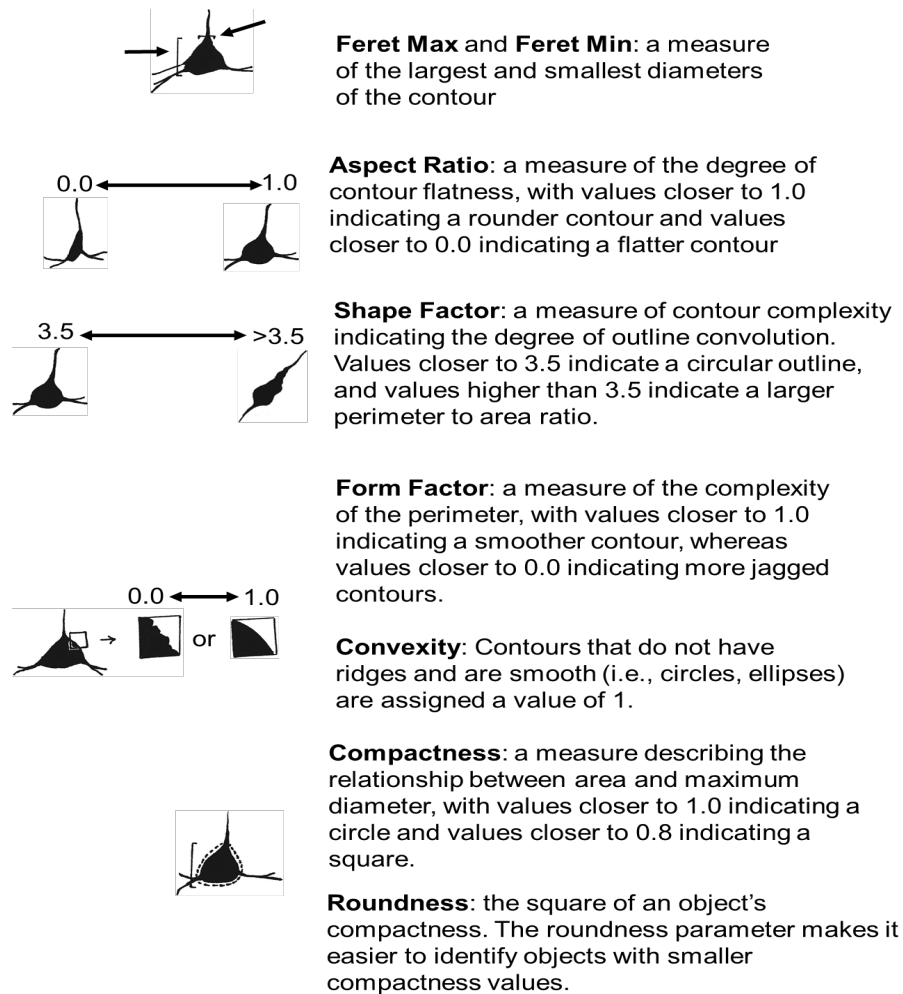


Figure 7: This chart represents the metrics used in measuring the soma body of each respective neuron. These metrics come from NeuroExplorer program (Adaptation *from*: A.C. Barrientos 2019 SFN poster)

Figure 8

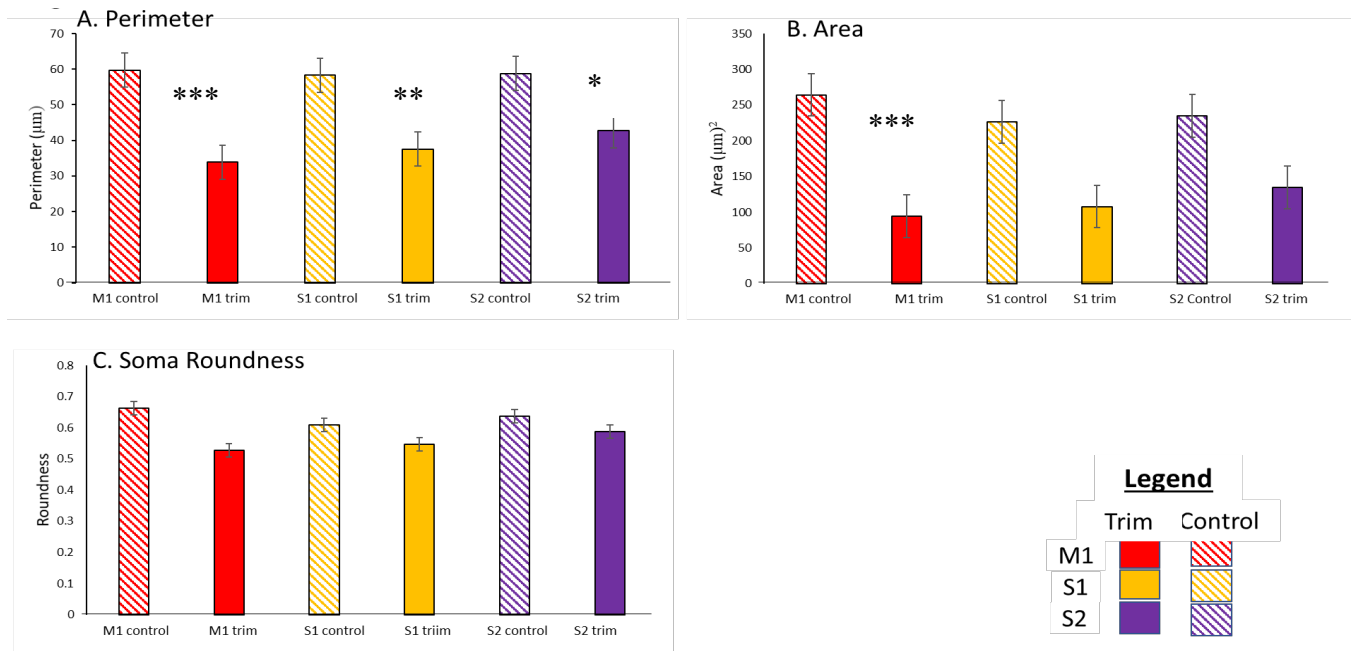


Figure 8: Perimeter, Area, and soma roundness bar graphs for the control and trim groups: The average values found from the (A) soma perimeter, (B) soma area and (c) and soma roundness for the control and trim groups. The x-axis indicates the type of cell and in the experimental group it belongs to. The Y-axis indicates the variable quantity for a given parameter. Bar graphs illustrate the population means with error bars representing the standard error of the mean.

Figure 9

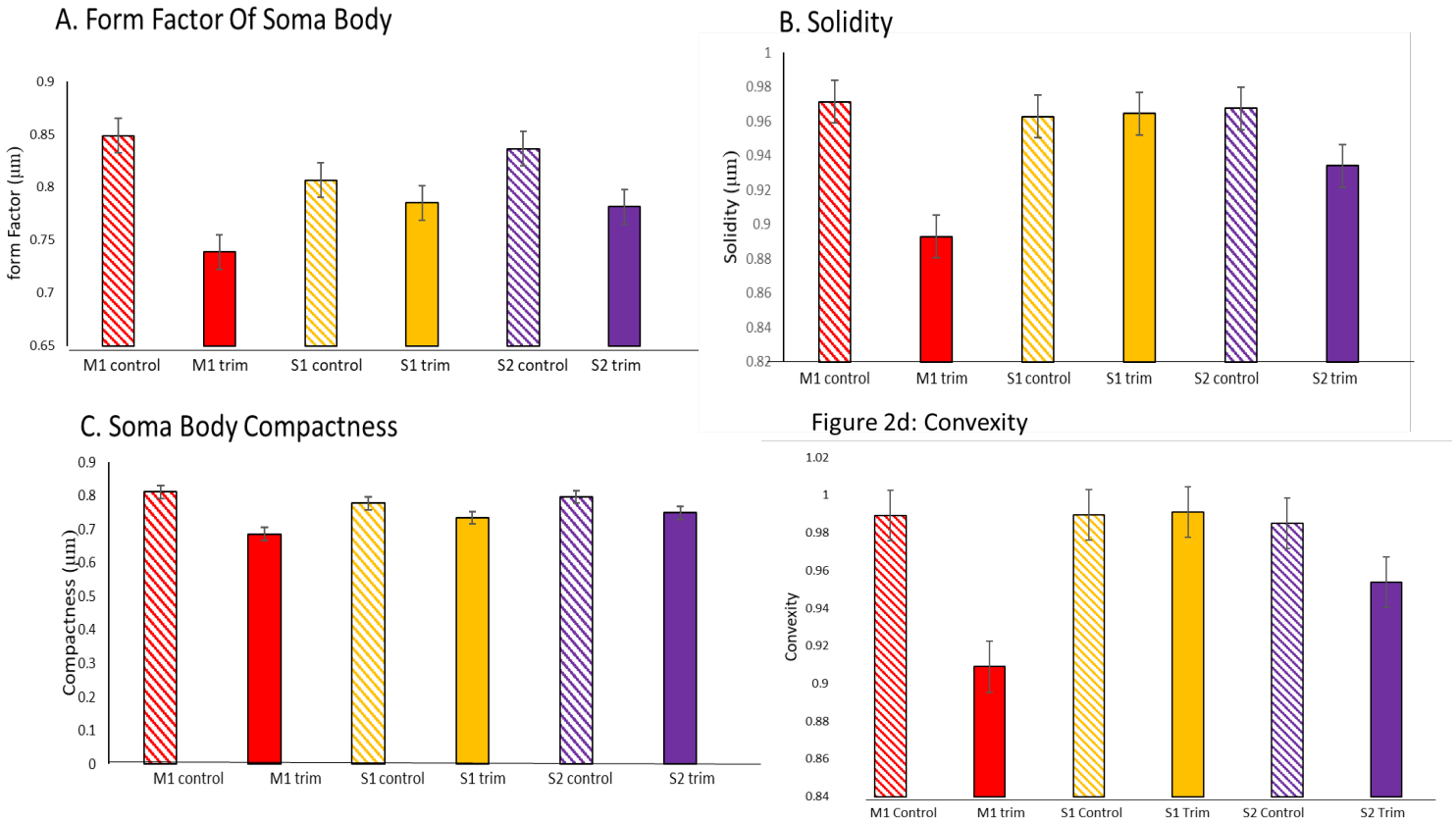


Figure 9: Form factor, solidity, compactness, convexity: The average values found from the (A) form factor, (B) solidity, (C) compactness, (D) convexity of the soma for the control and trim cell groups. The x-axis indicates the type of cell and in the experimental group it belongs to. The Y-axis indicates the variable quantity for a given parameter. Bar graphs illustrate the population means with error bars representing the standard error of the mean.

Figure 10

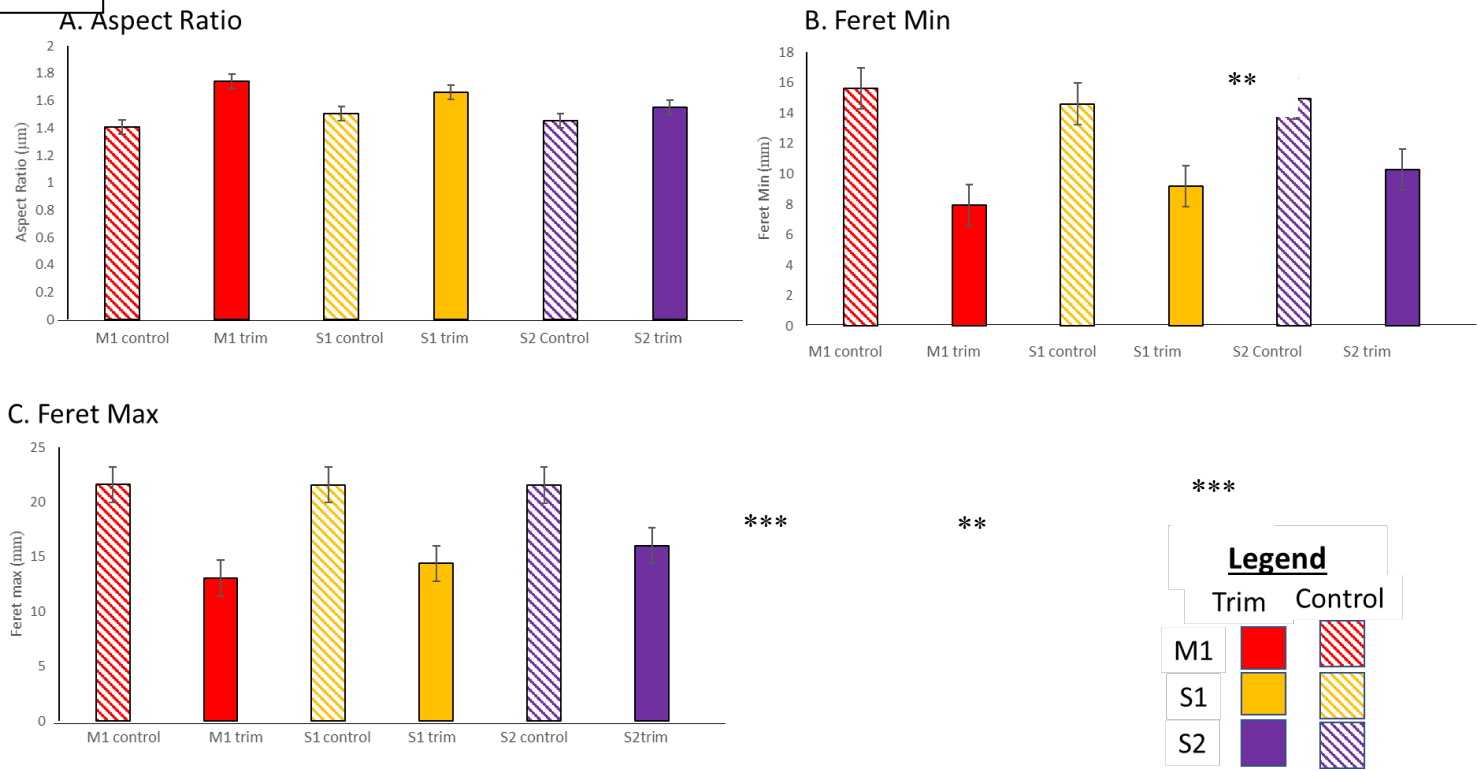


Figure 10: Aspect ratio, feret min, feret max: The average values found from the (A) aspect ratio, (B) feret min, (C)feret max of the soma for the control and trim groups. The x-axis indicates the type of cell and in the experimental group it belongs to. The Y-axis indicates the variable quantity for a given parameter. Bar graphs illustrate the population means with error bars representing the standard error of the mean.

Figure 11

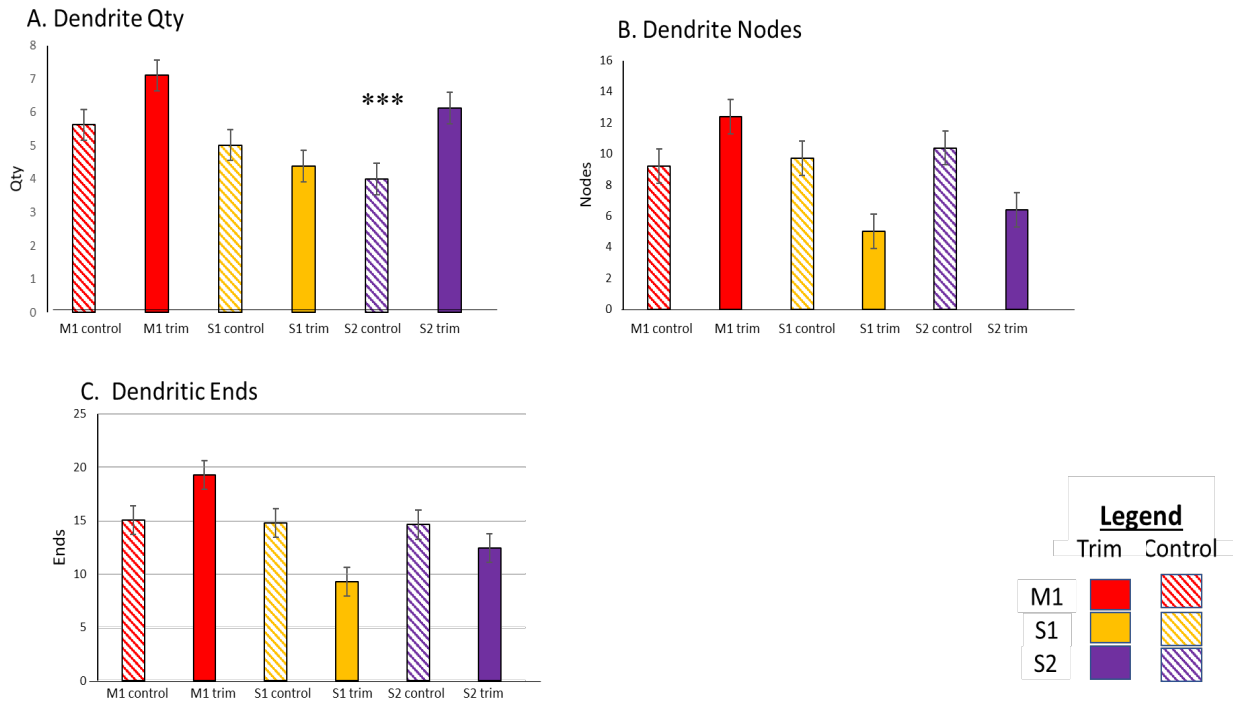


Figure 11: Dendrite quantity, dendrite nodes, dendrite ends: the average values found for the (A). Dendrite quantity, (B) dendrite nodes, (C) dendrite ends for the dendrites from the control and trim cells. The x-axis indicates the cell and which group it belongs to. The Y-axis describes the values for a given perimeter. Bar graphs each illustrate the population means with error bars representing the standard error of the mean.

Figure 12

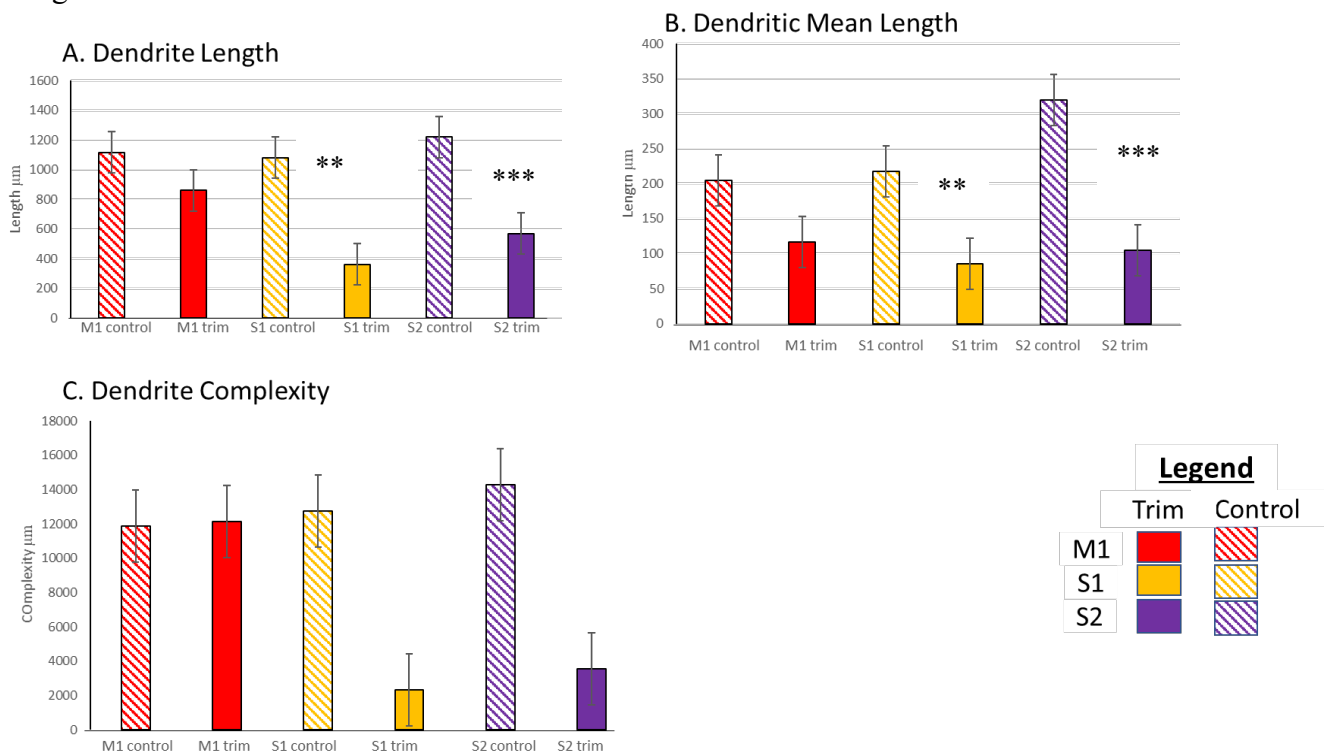


Figure 12: length, mean length, dendritic complexity: The average values found for the (A) Dendrite length (B) dendrite mean length and, (C) dendritic complexity for the dendrites from the control and trim cells. The x-axis indicates the cell and which group it belongs to. The Y-axis describes the values for a given perimeter. Bar graphs each illustrate the population means with error bars representing the standard error of the mean.

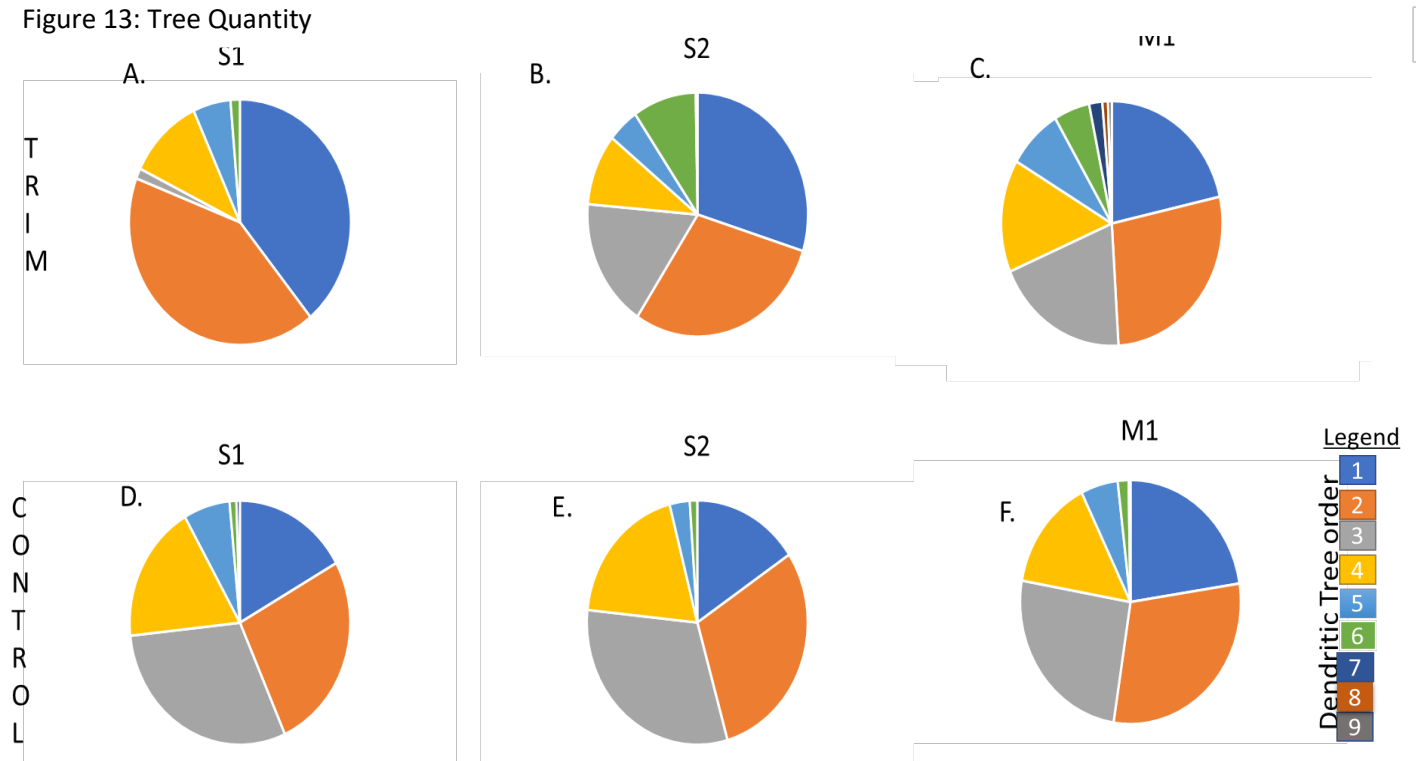


Figure 13: Tree Quantity: Depicts the quantity of dendritic trees there are in each order. Pie charts represents data in percent form and for the control and trim cell groups. Panels A and D shows the percent differences in dendritic tree orders for S1 cell in the control and sensory deprived groups. Panels B and E shows the percent differences in dendritic tree orders for S2 cell in the control and sensory deprived groups. Panel C and F shows the percent differences in dendritic tree orders for M1 cell in the control and sensory deprived groups.

Figure 14

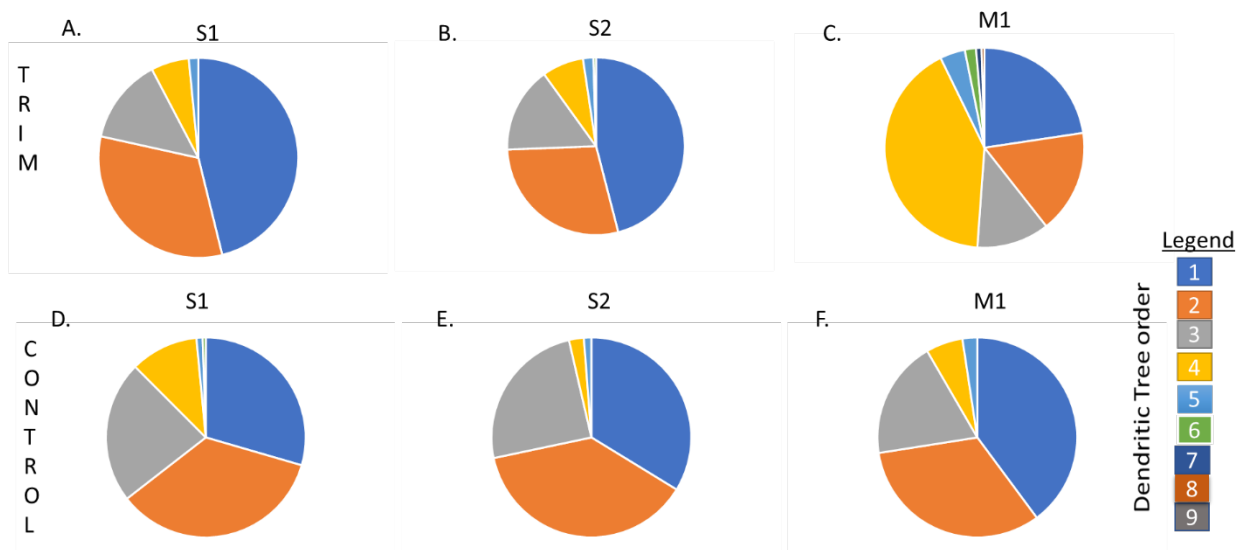


Figure 14 Tree Nodes: Depicts the tree nodes of dendritic trees there are in each order. Pie charts represent data in percent form and for the control and trim cell groups. Depicts the nodes of dendritic trees there are in each order. Pie charts represents data in percent form and for the control and trim cell groups. Panels A and D shows the percent differences in dendritic tree orders for S1 cell in the control and sensory deprived groups. Panels B and E shows the percent differences in dendritic tree orders for S2 cell in the control and sensory deprived groups. Panel C and F shows the percent differences in dendritic tree orders for M1 cell in the control and sensory deprived groups.

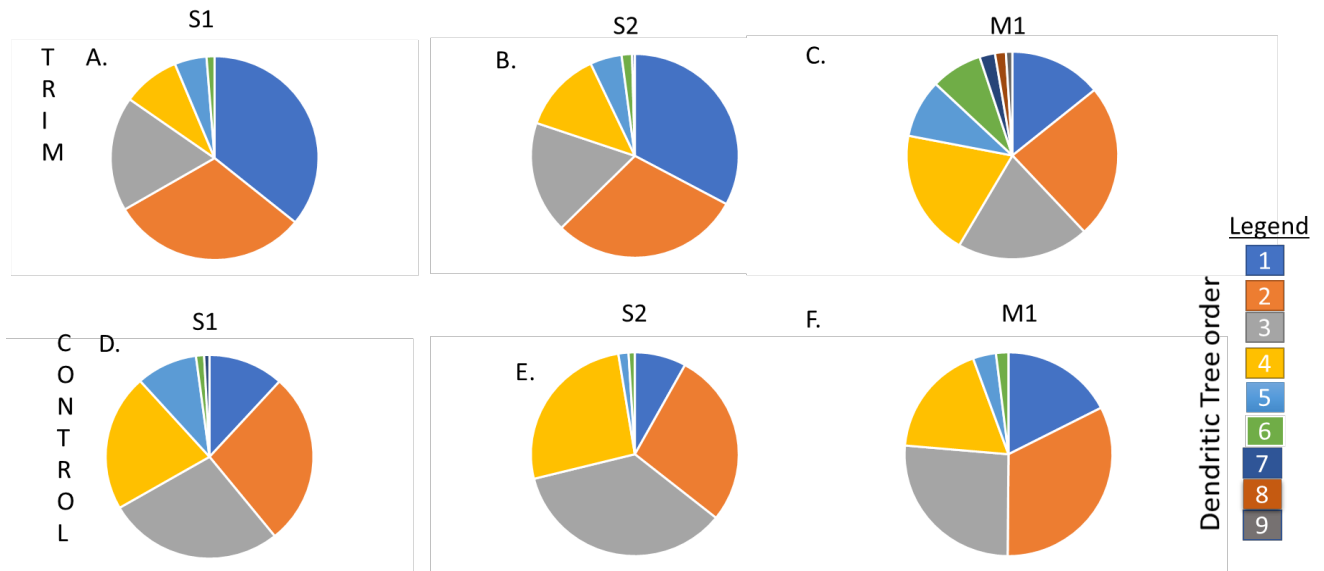


Figure 15 Total length: Depicts the tree length of dendritic trees there are in each order. Pie charts represent data in percent form and for the control and trim cell groups. Depicts the quantity of dendritic trees there are in each order. Pie charts represents data in percent form and for the control and trim cell groups. Panels A and D shows the percent differences in dendritic tree orders for S1 cell in the control and sensory deprived groups. Panels B and E shows the percent differences in dendritic tree orders for S2 cell in the control and sensory deprived groups. Panel C and F shows the percent differences in dendritic tree orders for M1 cell in the control and sensory deprived groups.

Neuronal Cell	N = 123
M1 Trim	13
M1 Control	29
S1 Trim	13
S1 Control	18
S2 Trim	34
S2 Control	16

Table 1 Neuronal population: the total number of cells used in the entirety of the experiment. categorized by cell type and experimental condition.

GROUP Means	Perimeter(μm)	Area(μm^2)	Feret Max(μm)	Feret Min(μm)	Aspect Ratio	Compactness	Convexity	Form Factor	Roundness	Solidity
M1 control	59.73	264.37	21.59	15.62	1.4	0.81	0.98	0.84	0.66	0.97
M1 Trim	33.86	94.08	13.05	7.95	1.74	0.68	0.91	0.73	0.52	0.89
S1 control	58.32	226.15	21.55	14.6	1.5	0.77	0.98	0.8	0.61	0.96
S1 Trim	37.54	107.97	14.39	9.2	1.65	0.73	0.99	0.78	0.54	0.96
S2 control	58.8	235.01	21.55	14.94	1.45	0.79	0.98	0.83	0.63	0.96
S2 Trim	42.7	134.56	16.03	10.27	1.55	0.74	0.95	0.78	0.58	0.93

Table 2 Group means of soma body measurements: Parameters of the soma body, perimeter, area, feret max, feret min, aspect ratio, complexity, convexity, solidity, compactness, form factor and roundness.

AREA	Qty	Nodes	Ends	Mean Length	Length(μm)	Complexity
M1 Control	5.62	9.2	15.03	204.5	1116.8	11880.87
M1 Trim	7.1	12.4	19.3	116.1	861.1	12131.8
S1 control	5.01	9.69	14.81	217.9	1080.98	12763.48
S1 Trim	4.38	5	9.3	85.38	363.72	2341.33
S2 control	4	10.37	14.6	319.9	1219	14265.4
S2 Trim	6.12	6.39	12.45	104.48	570.4	3560.2

Table 3 Dendritic group means: Parameters of the dendrite for the trim and control cells.

Focused on the metrics of quality, nodes, length, mean length, and complexity of the dendrites.